Detector Development for SNAP Dark Energy Space Mission Concept

Chris Bebek

18 October 2009

Detectors for Astronomy 2009

ESO Garching

Outline

- What is SNAP
- CCD development
- HgCdTe development
- Detector electronics
- Detector packaging
- Focal plane assembly

- Groups that have have participated in SNAP detector work
  - Caltech
  - Fermi National Accelerator Lab
  - GSFC / DCL
  - France IN2P3 Marseilles
  - France Lyons
  - JPL
  - LBNL
  - University of Michigan
  - RIT / RIDL
  - SLAC National Accelerator Lab
  - Space Sciences Lab / UC Berkeley
  - STScI / IDL
  - Yale

- and vendor work
  - Raytheon Vision Systems
  - Teledyne Imaging Sensors

What is SNAP?

- SNAP is a DOE dark energy space mission concept based, first proposed in 1999, and based heavily on Type Ia SNe.
- Starting in 2002, the US Dept of Energy provided support for concept development and instrument R&D.
- SNAP has evolved over the last 10 years to accommodate new measurement techniques – new collaborators with new ideas.
- Final incarnation is what I will be show here.

- SNAP is not JDEM.
- JDEM is a joint DOE–NASA effort by their respective project offices to come up with an affordable mission concept and implementation plan.

- The hope is that the work that I review here will help inform that decision making process.

Type Ia Supernovae Observables

- ~2000 Type Ia SNe by from repetitive scan of a small field.
- This automatically yields a time sequence of light curves.
- Acquire a spectrum at peak brightness.

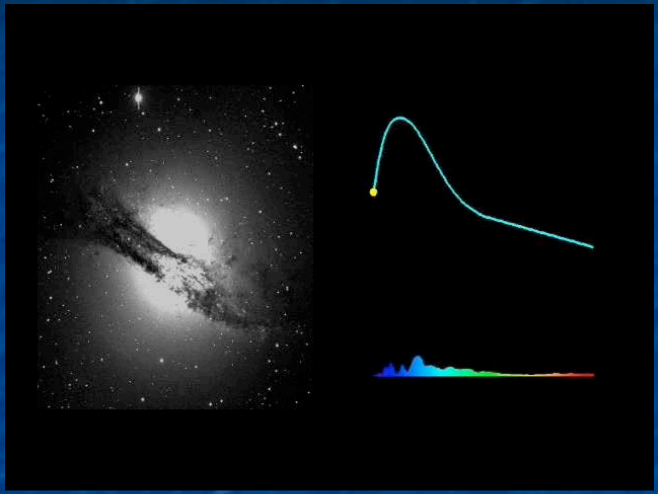

- The dark energy action is most evident below z ~1.5.
- Supernova spectral features fall in the range of 400–1700 nm.
- Multi-band photometry.

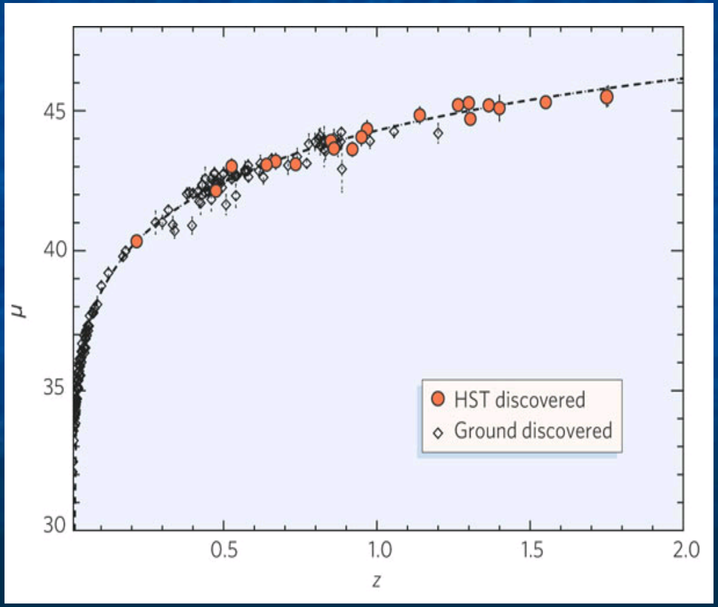

Weak Lensing Observables

- Measure the ellipticities of 100 of millions of galaxies to 0.001.
- Galaxy redshifts determined photometrically (5% precision) based on spectrographic redshift calibration for a few 10^5 galaxies.
- Form a power spectrum of ellipticity – ellipticity angular correlations.
- Most measurements done below 1000 nm, but NIR also valuable.
- NIR required to minimize *catastrophic* photo-z's.

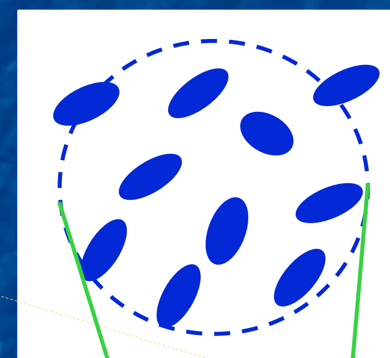

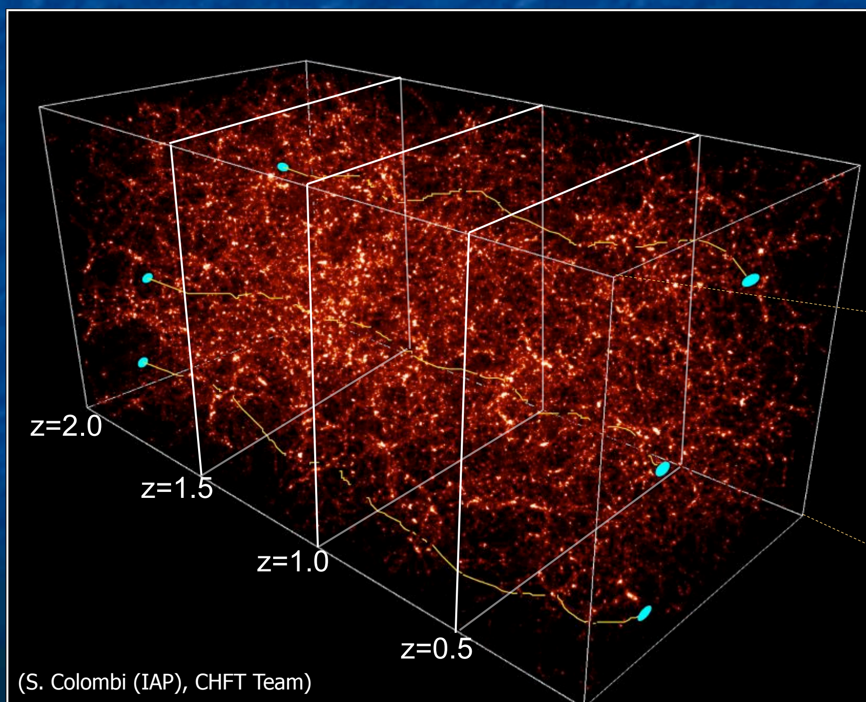

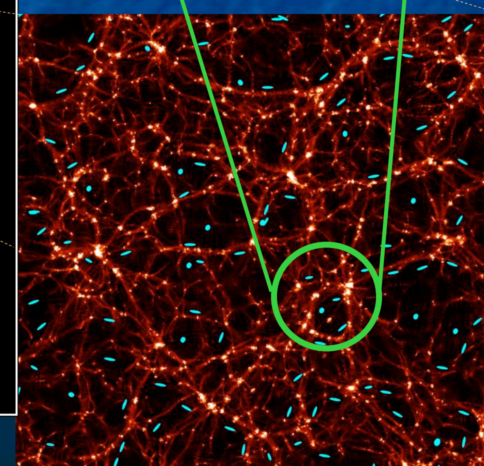

BAO Observables

Look for galaxies at a common redshift that cluster on an annulus.

The redshifts (0.3% precision) come from looking at emission lines.

The angular radius corresponds to the standard ruler (measurement along line of sight is also contains BAO signal).

Ha line measured with R~300 from 900–1700 nm.

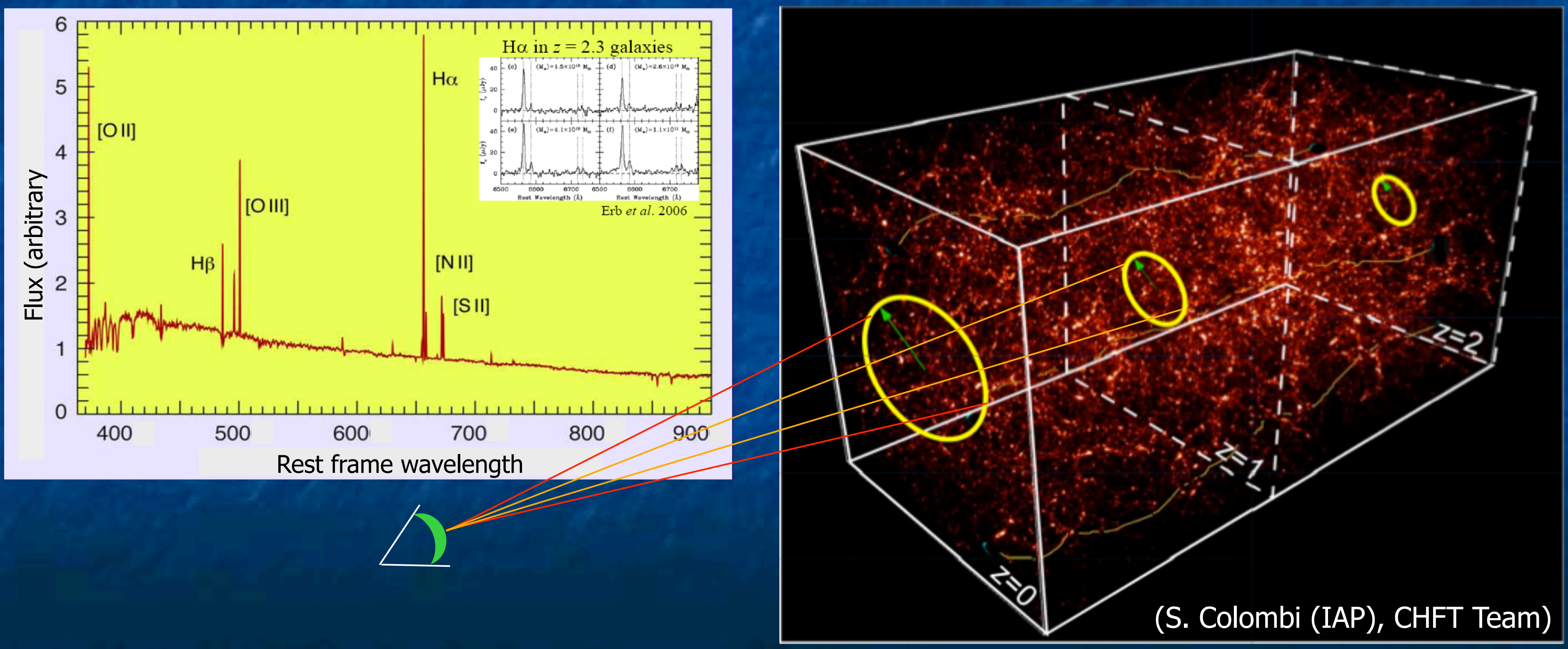

(S. Colombi (IAP), CHFT Team)

SNAP Satellite

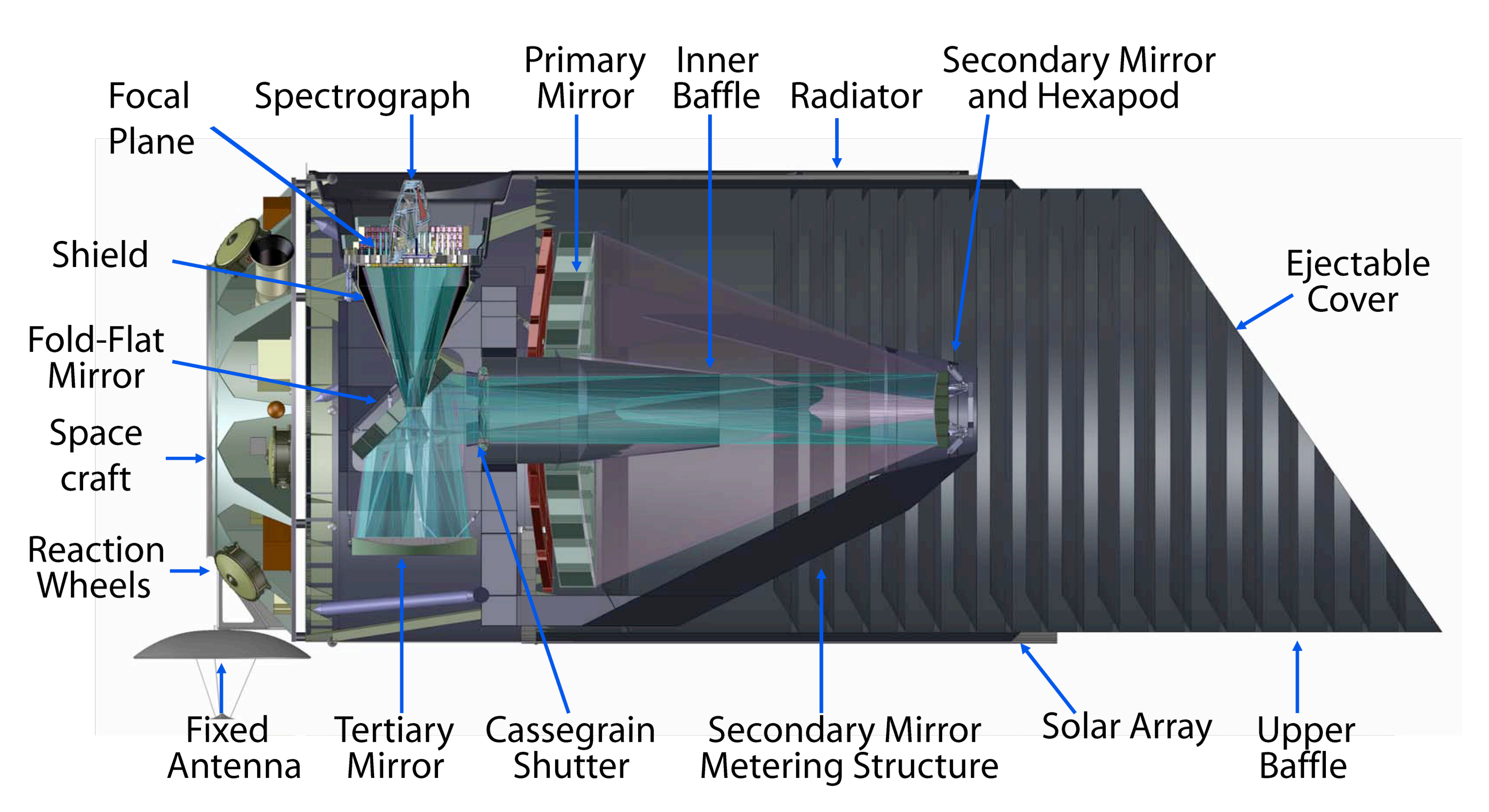

Focal Plane

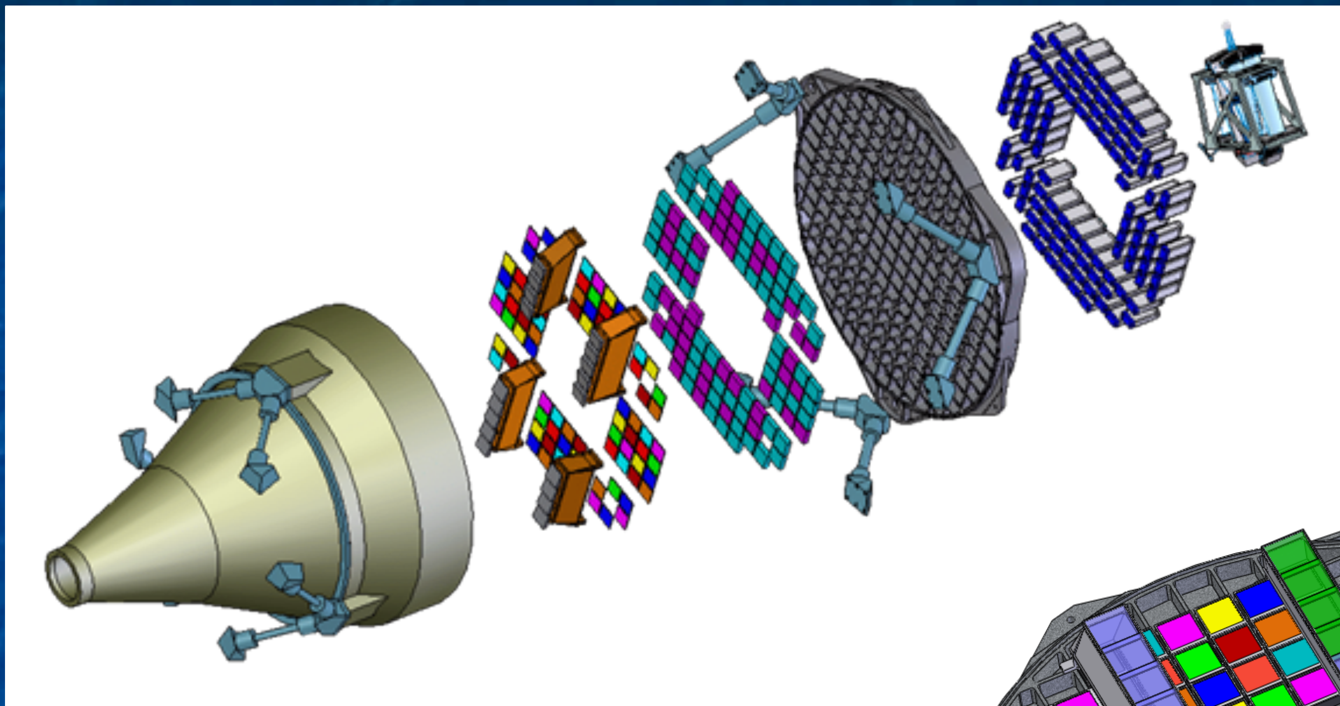

Detector	#
Imager CCD	57
Imager NIR	31
Guider	3
Spectro NIR	2

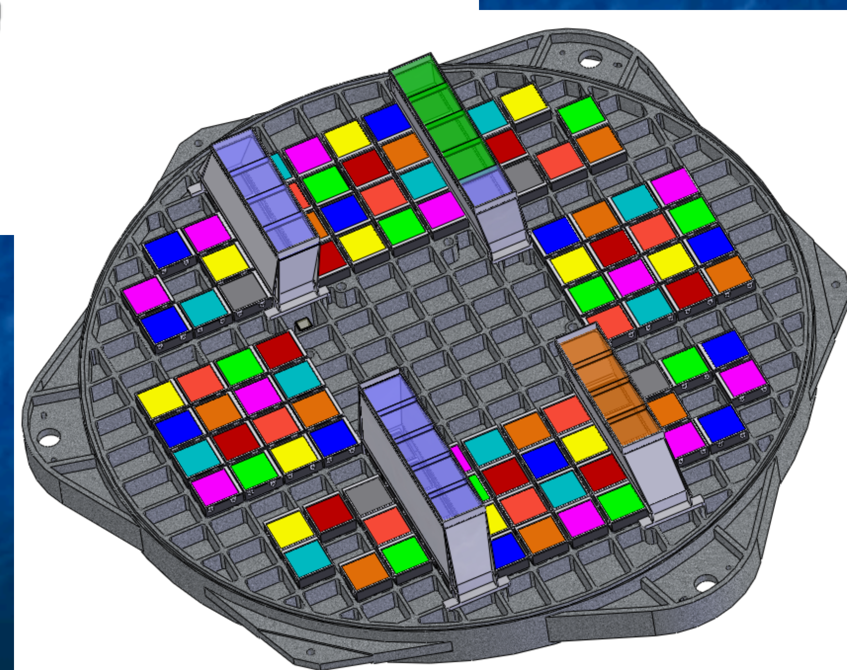

Deep Scan - SNe, WL and BAO

- SNe
  - Repetitive visits to same field.
  - Discovery and follow up.
- WL and BAO
  - Photo-z calibration
  - Observation in filters and grisms.

- Note that intermixing of NIR and CCDs is required.

Survey	Area [deg^2]	Point Source [AB$_{mag}$]	$r_{1/2}$=0.3" Galaxy [AB$_{mag}$]	Emission Line Threshold	Resolved Galaxies
Deep	3.4	30.7	29.6	0.55	2×10^5
Wide	10,000	27.1	26.0	18.4	2×10^9

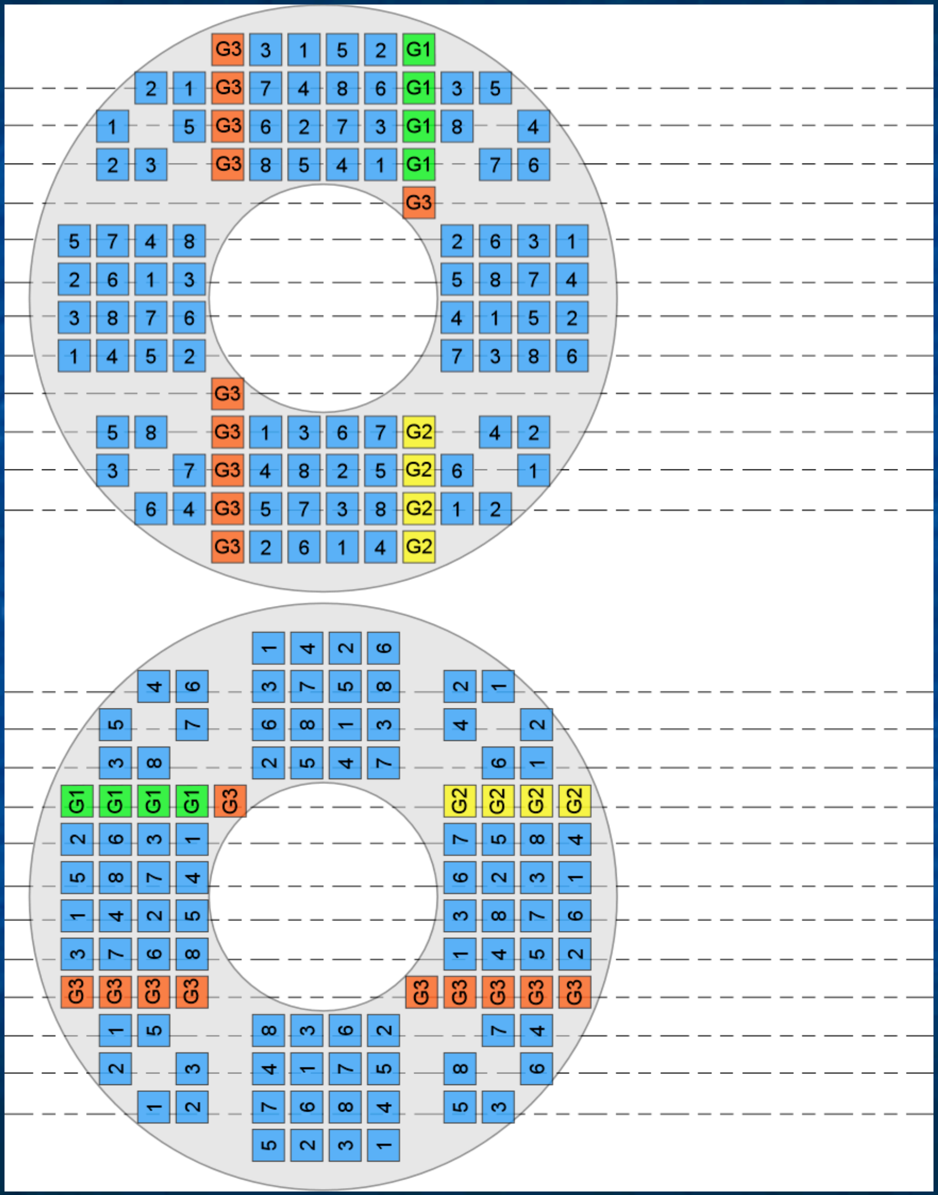

Wide, Filled Scan – BAO and WL

SNAP

Survey	Area [deg^2]	Point Source [AB_{mag}]	$r_{1/2}$=0.3" Galaxy [AB_{mag}]	Emission Line Threshold	Resolved Galaxies
Deep	3.4	30.7	29.6	0.55	2×10^5
Wide	10,000	27.1	26.0	18.4	2×10^9

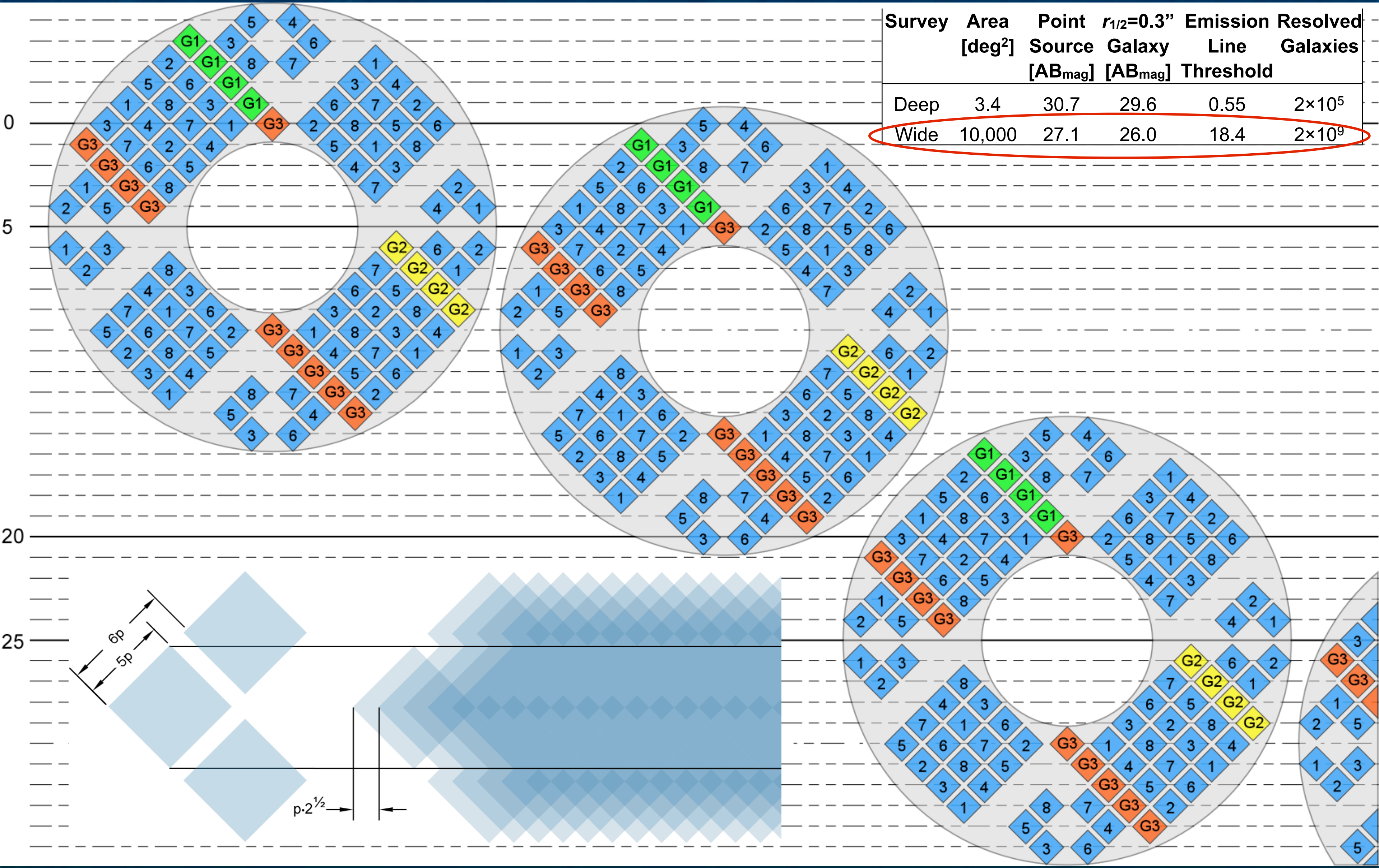

Detector Development Drivers

- CCD and NIR on same focal surface.
- CCD and NIR operate at the same temperature.
- Must be interleaved in any order.
- Focal must be easy to integrate.
- PSF is undersampled by 1.5-2
  - Maximize sky coverage with the available pixels.
  - Pixel response uniformity must be well understood for modest dithering to recover spatial information.
- Telescope and other satellite components are at room temperature - thermal photon impact on NIR.
- Radiation environment of an L2 orbit.
- Survive a 6 year mission lifetime.

Detector Goals

Parameter	
Instrumented FOV	1.13 deg^2
Wavelength response	380 – 1700 nm
Filter Set	8 bands, width R >4
Exposure time	200 − 300 seconds
Readout time	<30 seconds
Stray Light	<10% zodiacal

Optical Telescope Assembly	
Aperture	1.8 m
Focal ratio	f/11
Plate scale	
Visible	0.11 arcsec/pixel
NIR	0.18 arcsec/pixel

Focal Plane Assembly	
Flatness	
Visible	±20 μm
NIR	±40 μm
Temperature	120–140K

CCD Imaging Detectors	
Detector number	57
Pixel size	10.5 μm
Quantum efficiency	85% average
Read noise	3 e
Dark current	0.05 e/pixel/sec

NIR Imaging Detectors	
Detector number	31
Pixel size	18-20 μm
Quantum efficiency	80% average
Total noise	8 e

Trackers	
Detectors	3 NIR

Grisms	
Number	8 CCD and 10 NIR
Passband	0.4 – 1.7 μm
Number of passbands	3

Spectrograph	
Field of view	3 × 6 arcsec^2
Resolution (λ/Δ λ)	200 visible; 70 NIR
Exposure time	10 – 3000 seconds
Detectors	2 NIR

Detector Technologies Explored

CCD

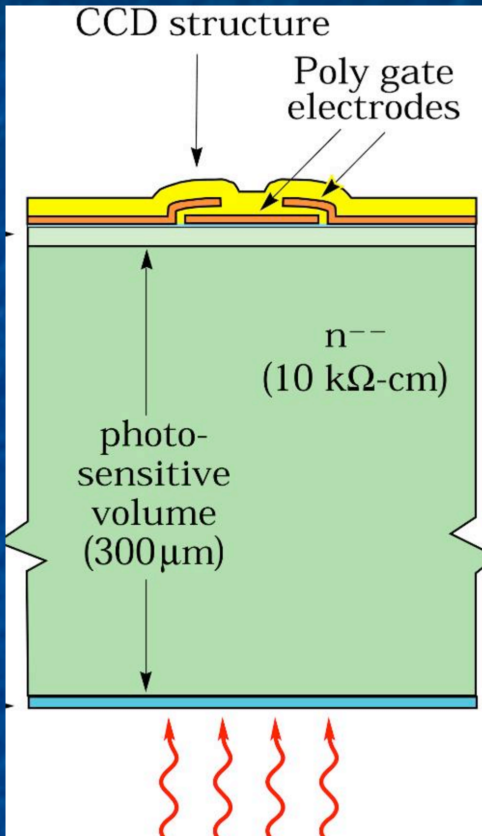

- p-channel devices
- Thick
- Back-illuminated
- Fully-depleted

Hybrid Pixels

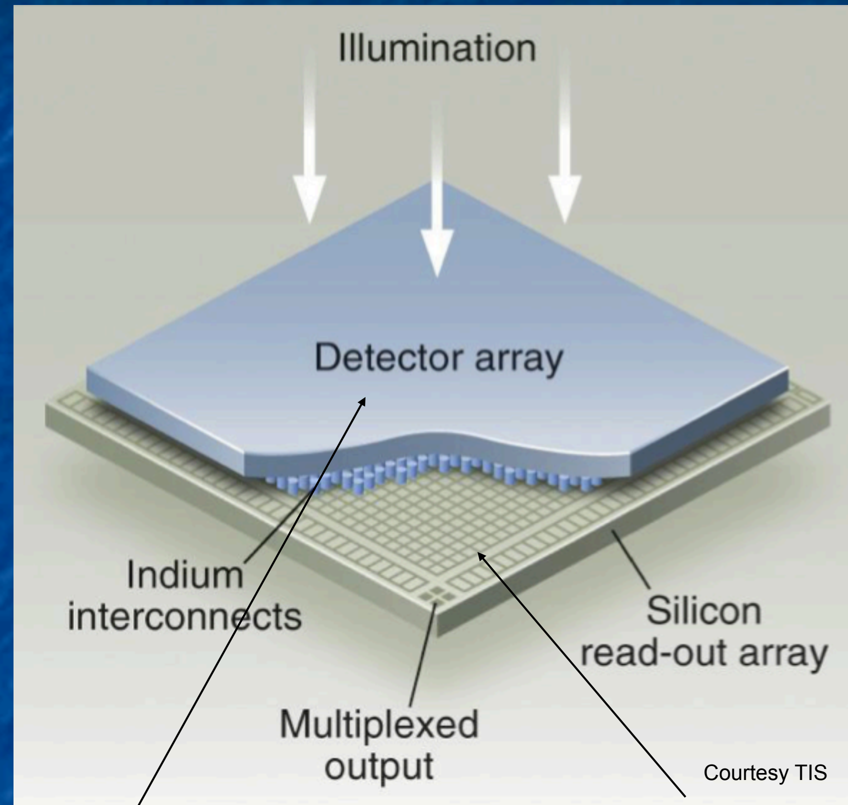

Detector material

- Silicon
- LPE HgCdTe 1.7 μm
- MBE HgCdTe 1.7 μm
- InGaAs 1.6 μm

Detector readout

- Raytheon 1k x 1k 20 μm
- Raytheon 2k x 2k 20 μm
- Teledyne 1k x 1k 18 μm
- Teledyne 2k x 2k 18 μm
- Teledyne 4k x 4k 10 μm

Detector Characterization – Big Picture

Photometry

- Quantum Efficiency
  - Monochromater and reflectometer setups
- Total noise – read noise plus dark current
  - Fowler and sample up the ramp
  - Imaging exposures – 200-300 s
  - Spectroscopy exposures – up to 10 ksec
- Fluence dependent gain - linearity
- Flux dependent gain
  - 5 decade calibrated light source
- Pixel Response Non-Uniformity
  - High statics autocorrelation analyses
  - Pin hole projectors
  - Hough transform pattern recognition

Shape Reconstruction

- Inter Pixel Capacitance
  - Auto-correlation method
  - Pin hole projector
  - Single pixel reset
- Persistence
  - Flat and dark sequences to map persistence time scale
  - Working device model to explain
- CTE radiation effects
  - Extensive proton radiation testing to measure charge transfer efficiency
  - Computer modeling of impact on weak lensing
  - Lessons learned applied to COSMOS data
- Lateral charge diffusion
  - Pin hole projector

Note: I cannot talk about all this.
A list of published articles is attached.

Visible

LBNL CCD Technology

(see N. Roe talk)

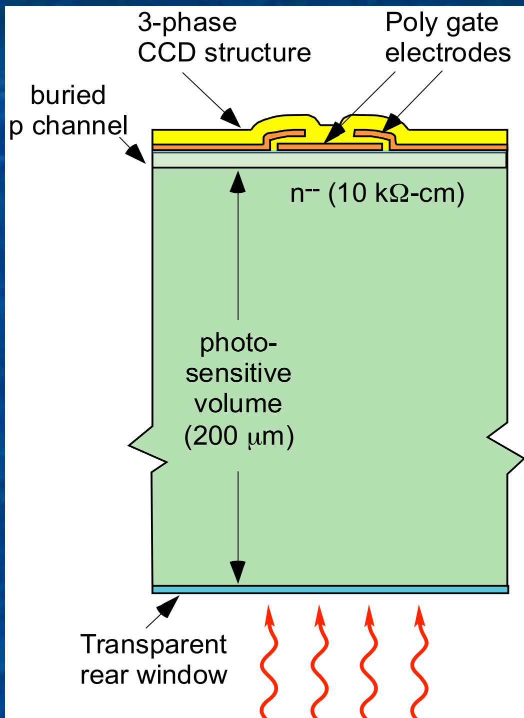

Thick device → extended wavelength response to 1000 nm.

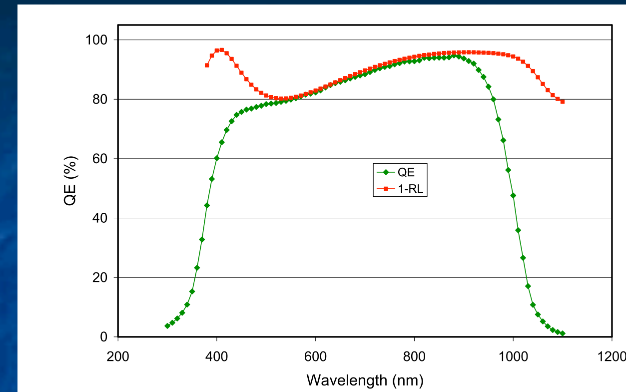

Hi-rho over depletion → small lateral charge diffusion, thus small pixels possible.

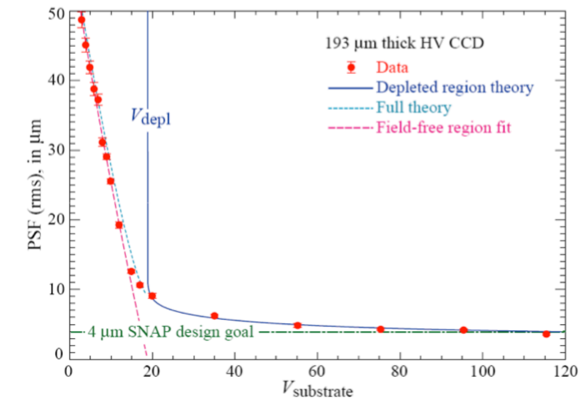

Hi-rho n-type silicon → improved radiation tolerance.

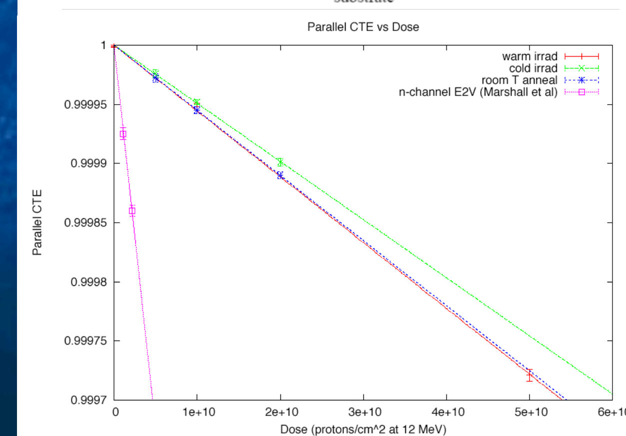

LBNL CCD technology

- Thick
- Fully/over depleted
- Back-illuminated
- n-type high resistivity silicon
- p-channel

SNAP CCD

3508 x 3512, 10.5 μm
(area matched to NIR)
200 μm thick
Four corner readout

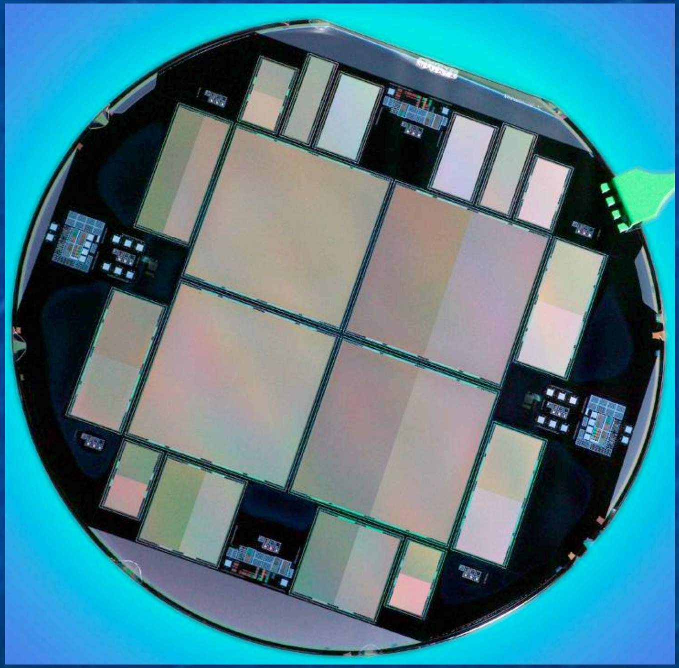

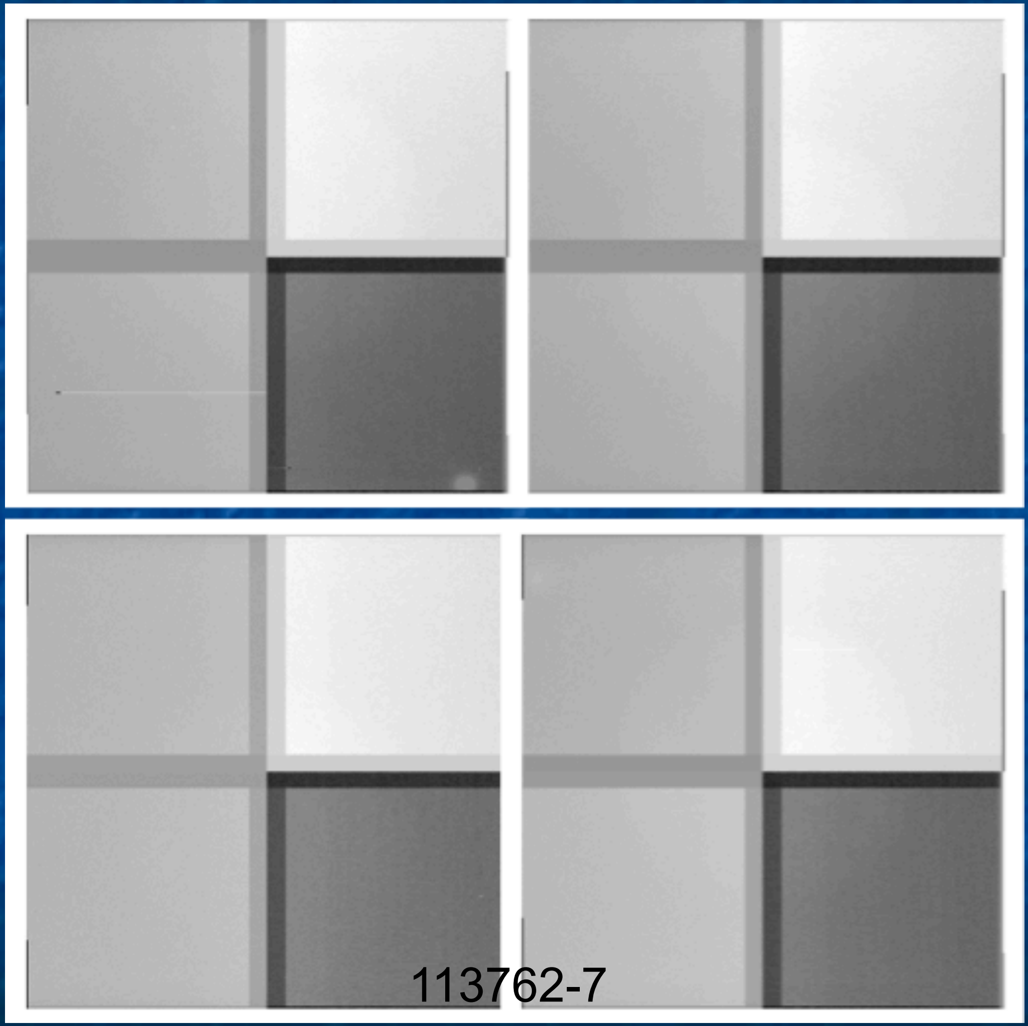

Cold probe data of four die on fully processed wafer

QE / Reflectivity Measurements

Simple red optimized AR coating

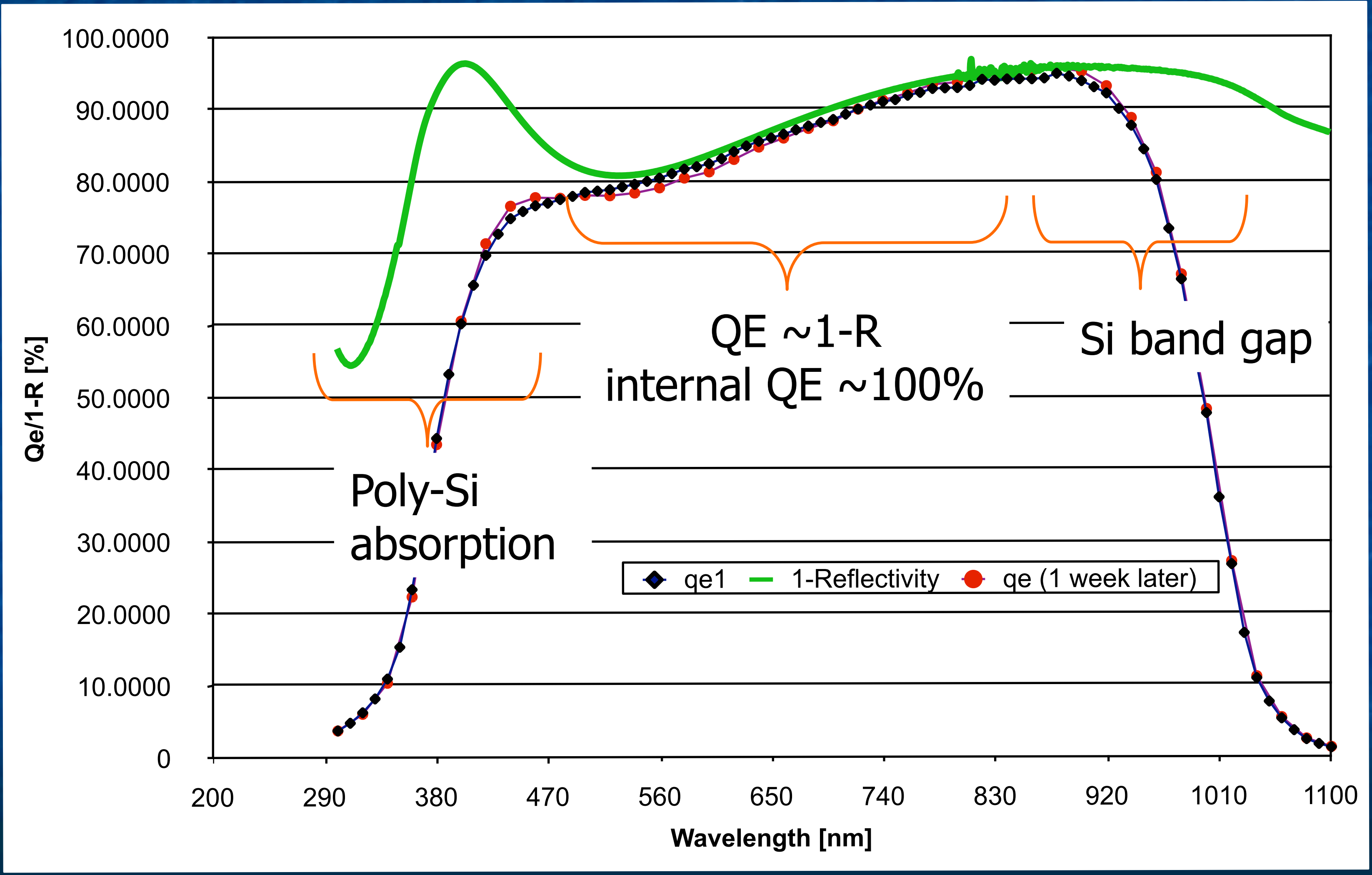

(see D. Groom talk)

Pixel Size Variation

- Deep co-added flats.
- Brightness spatial power spectrum along rows and columns.
- Identify random and coherent components.

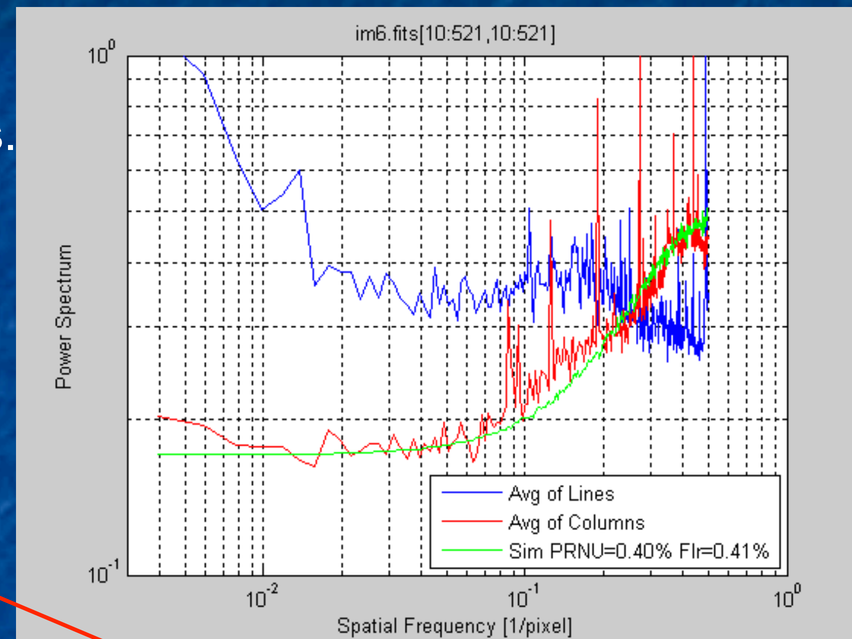

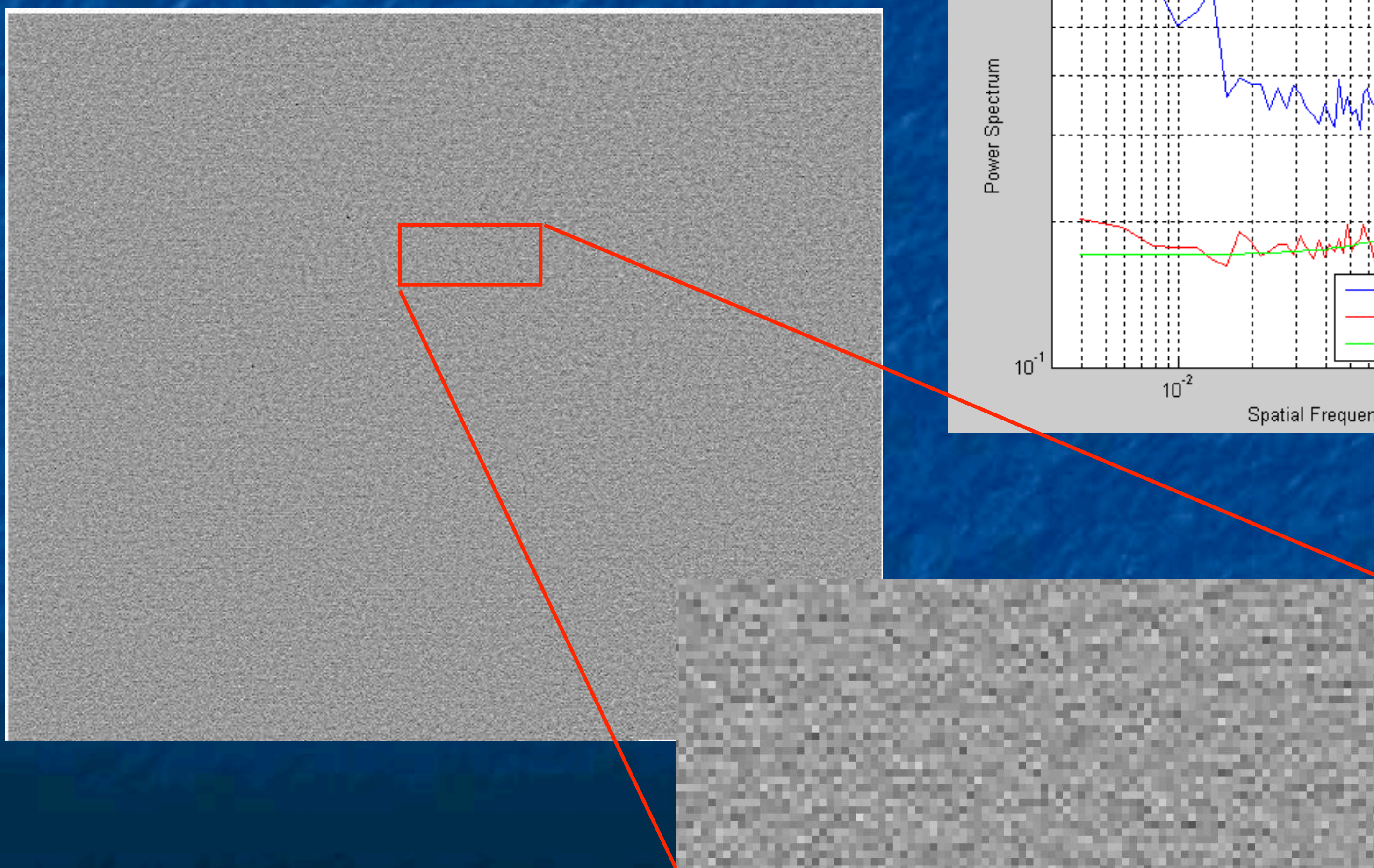

Lateral Charge Diffusion

- Photo-charge diffuses laterally during drift to pixel collection area.
- Over-depletion reduces the diffusion.
- 1 µm pinhole measurements confirm the theory.

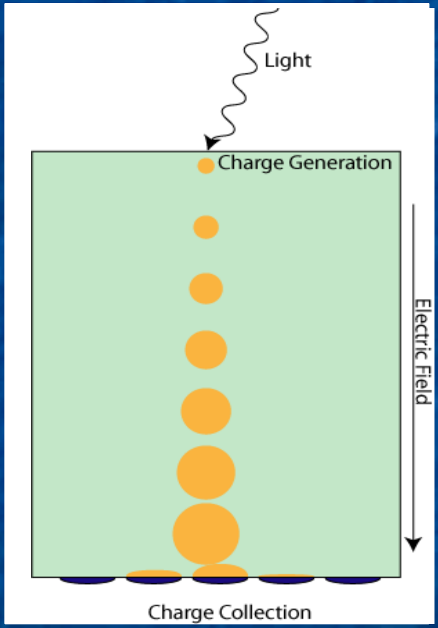

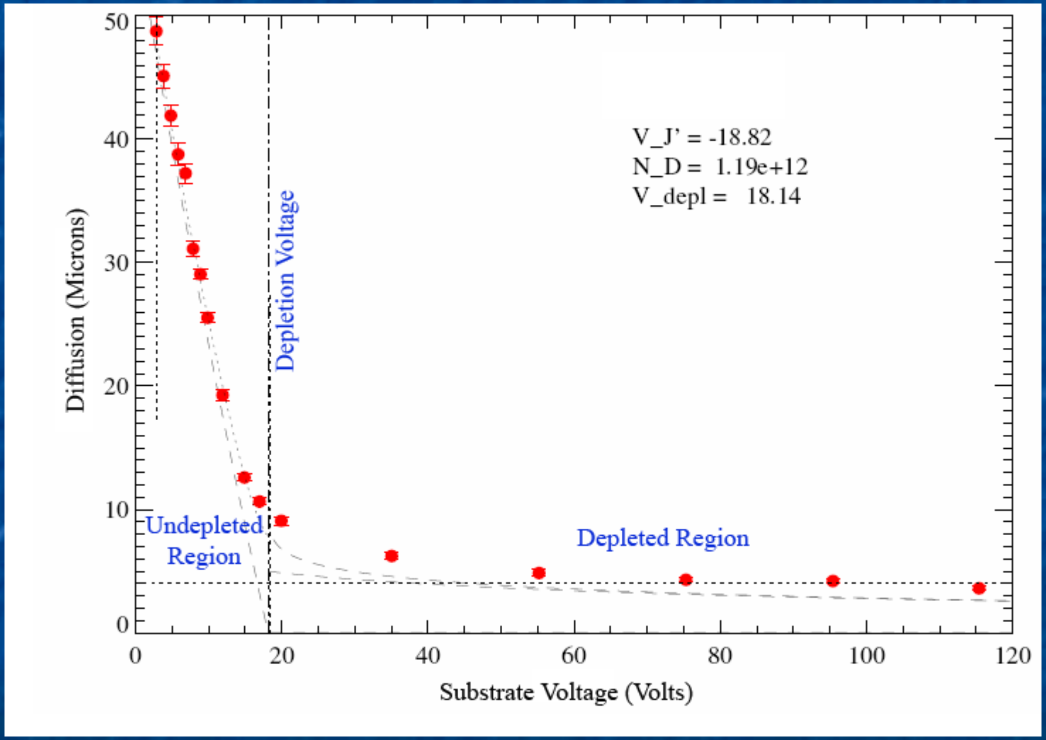

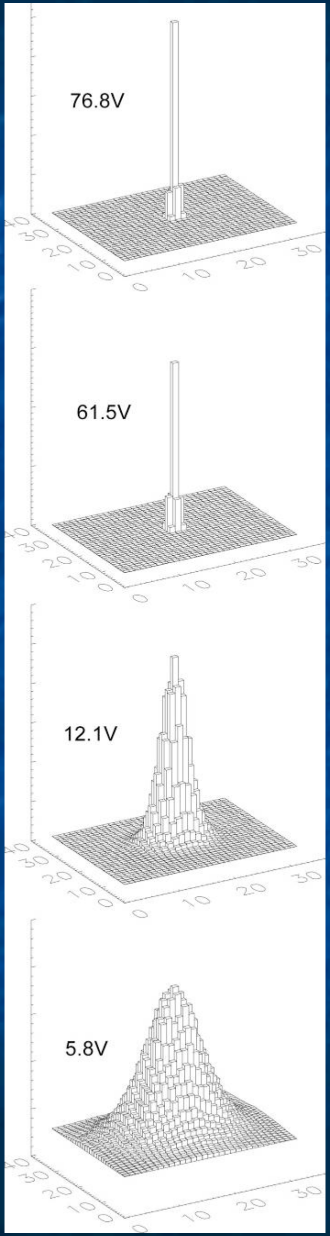

10.5 μm pixel make sense!

Radiation Tolerance

- Was postulated that p-channel CCDs are intrinsically more radiation tolerant
  - n-channel CCDs form phosphorous vacancy (P-V) defect that reduces CTE.
  - Boron-doped p-channel forms a di-vacancy defect (V-V), a second order process.
- We find a x10 improvement in CTE degradation vs proton dose relative to ACS, operated under their respective conditions.
- Detailed proton radiation studies using the LBNL 88” Cyclotron.
  - Hot pixel formation rate.
  - Dark current.
  - Study mitigating affects of sky level and leading charge density.

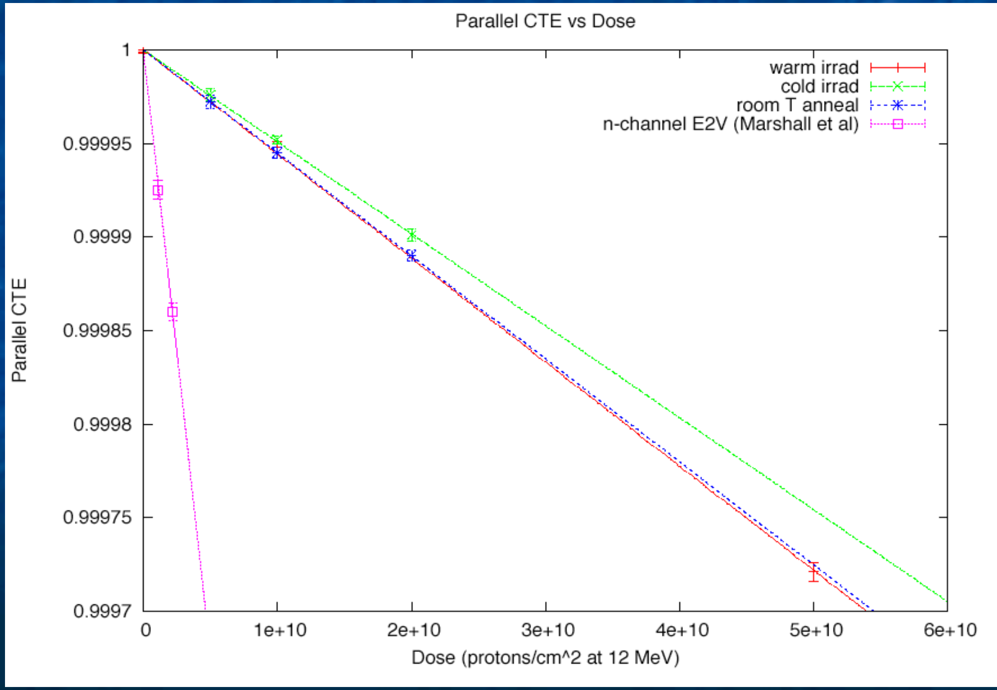

Hot pixels, dark current, background effects

- Hot pixel formation rate at least 10 times lower than for WFC at same threshold.

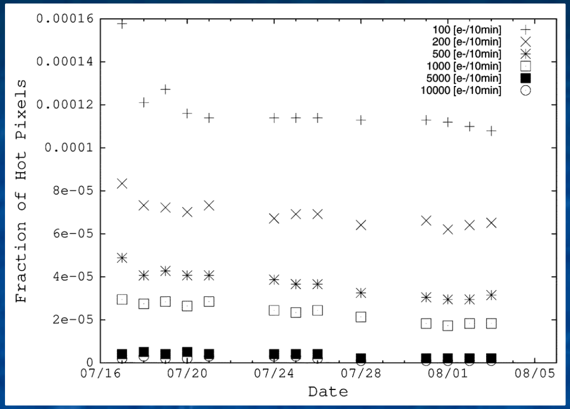

- Dark current increase is acceptable.

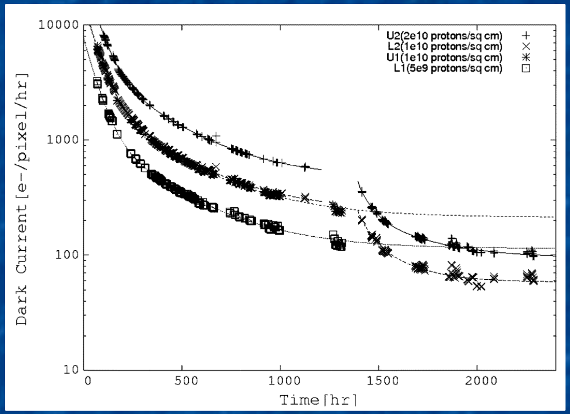

- Dependence of CTI on sky level and density of x-ray events for both the parallel and serial CTI after exposure to 2 x 10^{10} protons/cm^2.

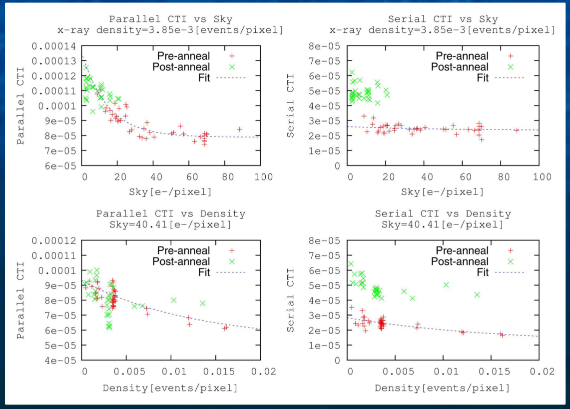

Radiation Interpretation

- We estimate the CTI at the end of 6 years by combining:
  - Measured CTI vs Non-Ionizing Energy Lose dose (proton irradiation).
  - Estimated NIEL dose behind shielding from satellite model (SPENVIS + shielding).
    - Obtain total expected NIEL dose of 6.6×10^6 MeV/g(Si) at 95% CL.
    - This is equivalent to 7×10^8 12.5 MeV protons.
  - Measured CTI dependence on background and event density.
  - Estimated zodiacal background at 400 nm and cosmic rays.

- Result:
  - Serial CTI degradation = -0.000 002; CTE = 0.999 997
  - Parallel CTI degradation = -0.000 003; CTE = 0.999 996 ($0.999\,996^{1750}$ = 99.3%)

NB This is for Q=1620 e; CTI scales as $1/Q^{1/2}$.

Near InfraRed

HgCdTe

- SNAP is a warm telescope – black body radiation runs away > 1.7 μm.
- Development effort focused on 1.7 μm cutoff material
  - Can operate at 130–140K with low enough dark current.
  - Complements the CCDs, which operate well in this temperature range.
- Multi-vendor, multi-technology detector development cycle.
- Of late, we have concentrated on Teledyne H2RG HgCdTe (2k x 2k, 18 μm) - five lot runs.
- Four of eight assemblies on SNAP-designed SiC mount are shown.

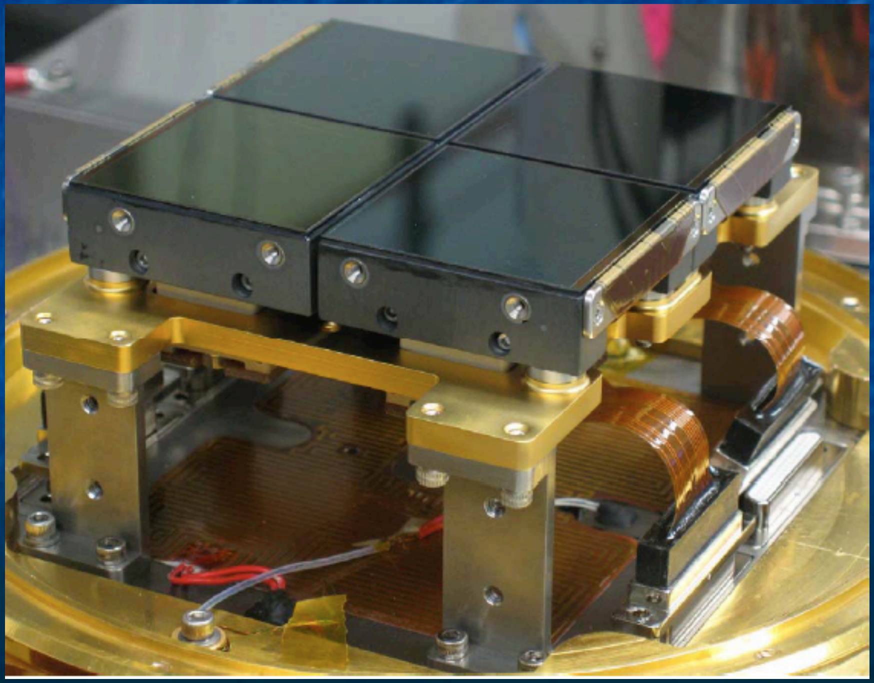

Total Noise

Total noise for imaging

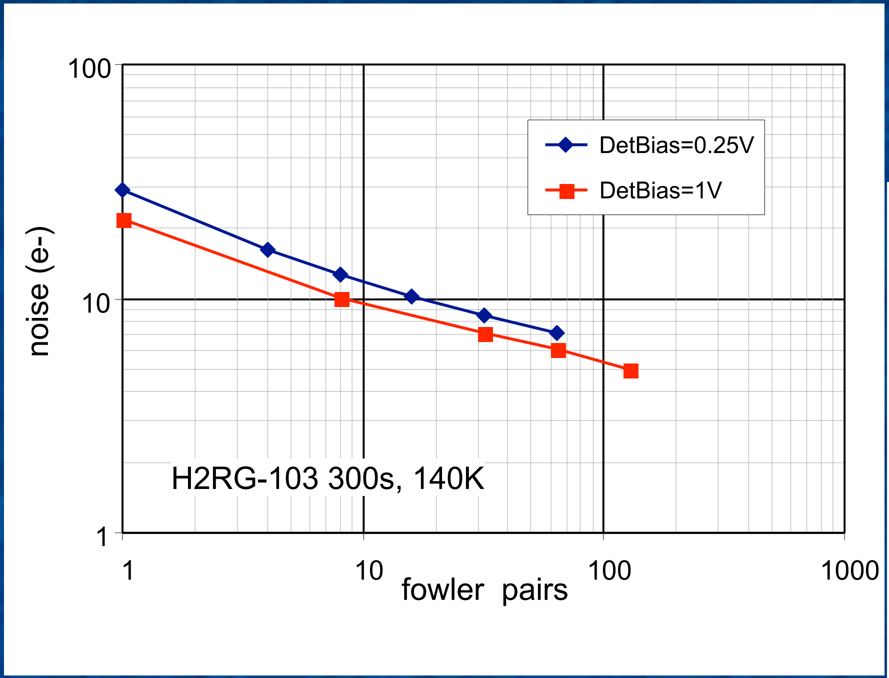

Total noise for spectroscopy

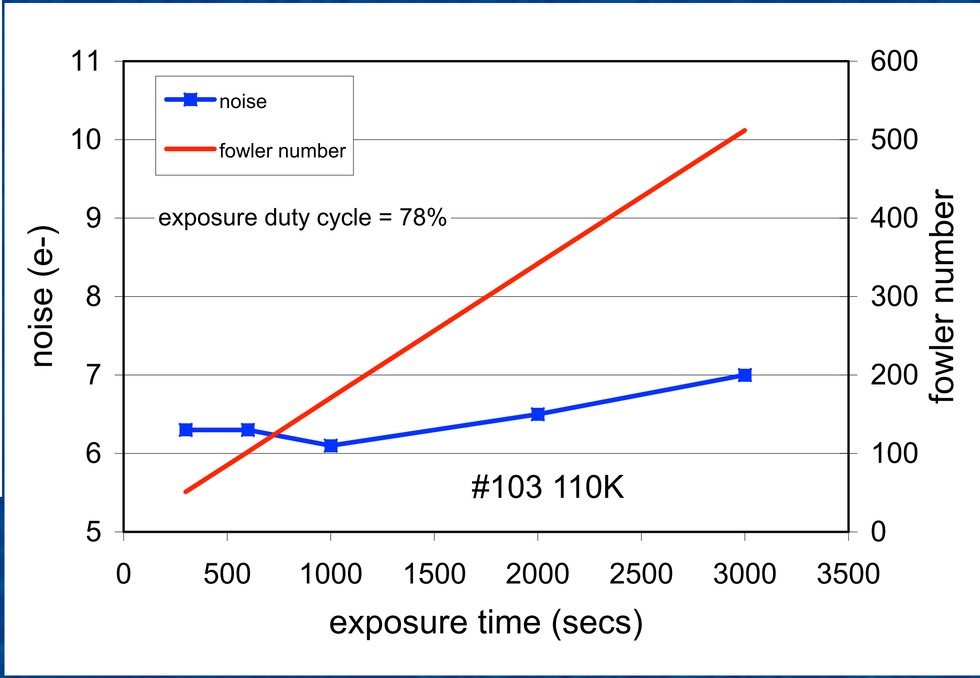

Improving readnoise has been the single struggle with these devices.

On-going for reduced noise for extremely long exposures (see C. Cerna poster).

QE and Charge Collection

- Quantum efficiency
  (see M. Schubnell talk)

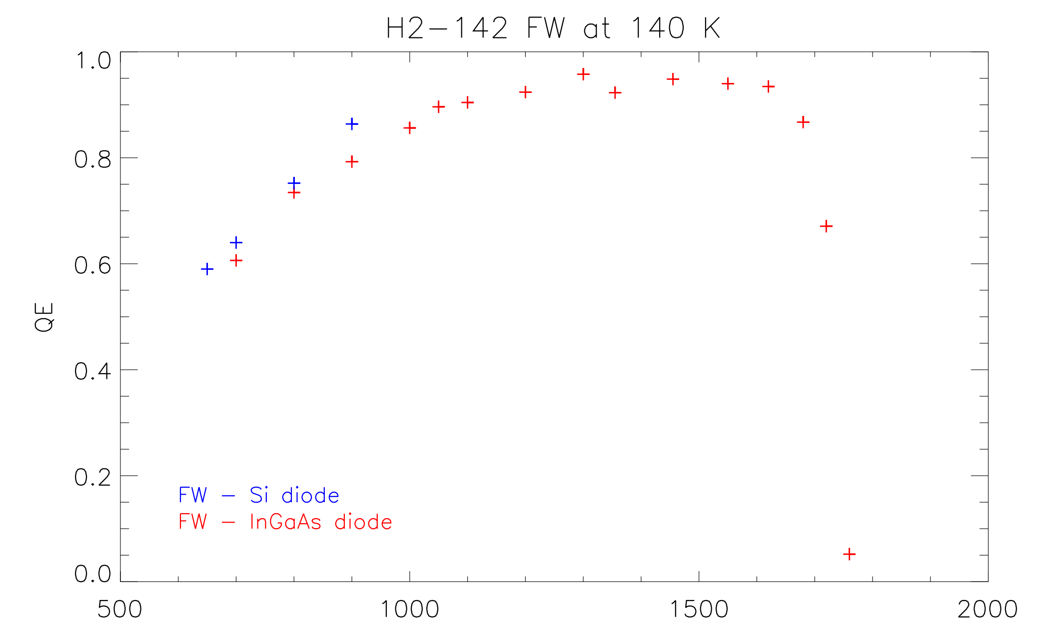

- Pin hole illumination scan for internal pixel structure
  (see T. Biesiadzinski talk)

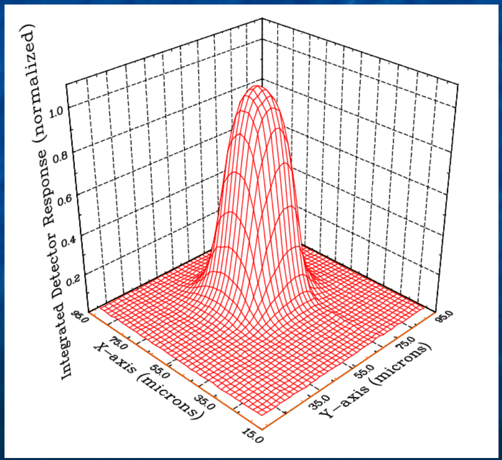

Single pixel pinhole scan

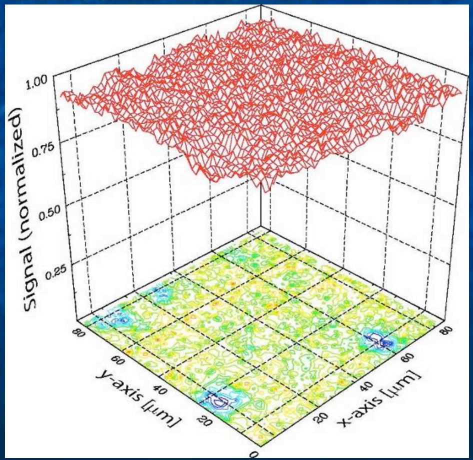

4x4 pixels sum

Pixel Size Variation

- Co-add many flats to get to equivalent of 10^6 e to be sensitive to effects at the 0.1% level.
- For small region, do Hough transform along 180 orientations (1 degree rotations).
- Look for correlation patterns.
  - Negative Correlation of adjacent pixels (small scales) suggests pixels size variations (~0.8% size variations)
  - Some structure on an 8 column pitch.
  - Scratch identification?

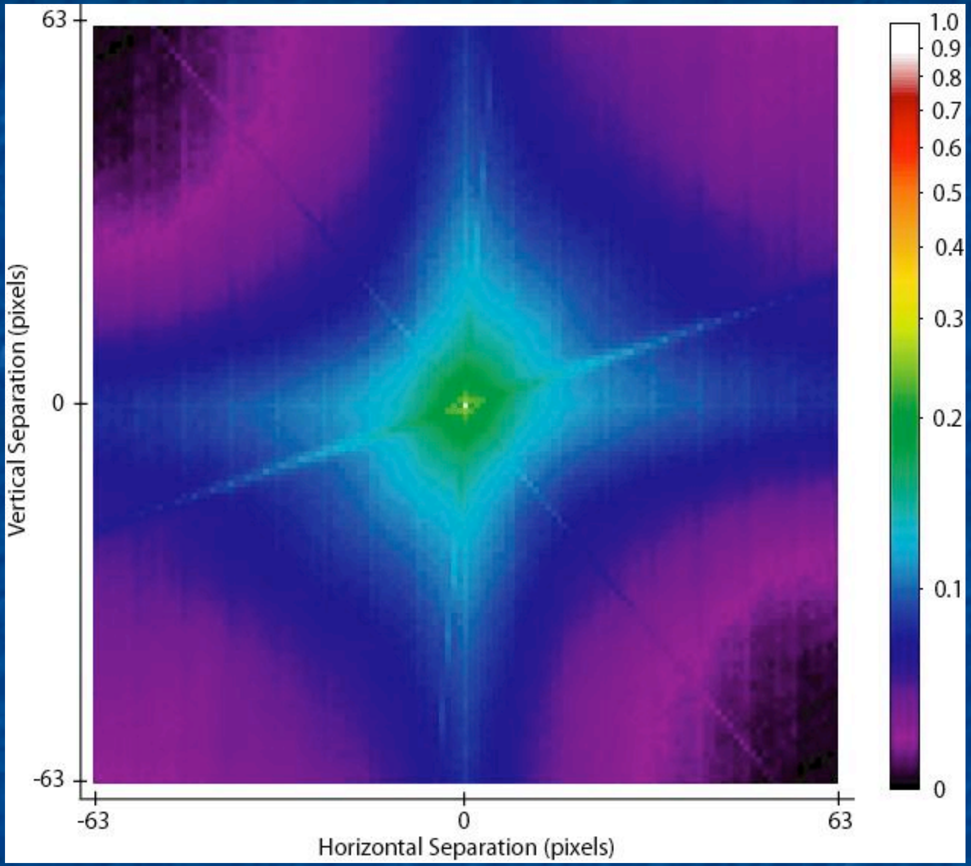

FPA 103 Correlation Function: -1 is totally anti-correlated, +1 is totally correlated).

Interpixel Crosstalk

- Pinhole optical stimulus

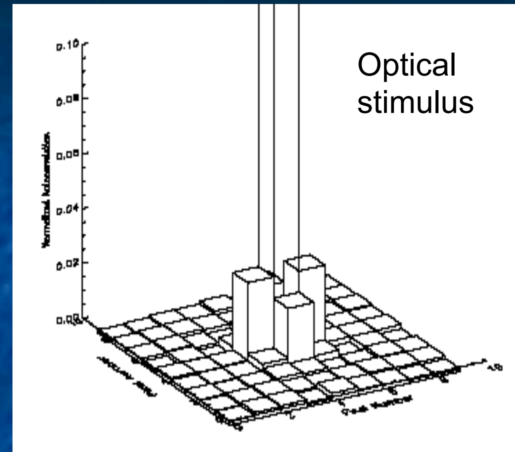

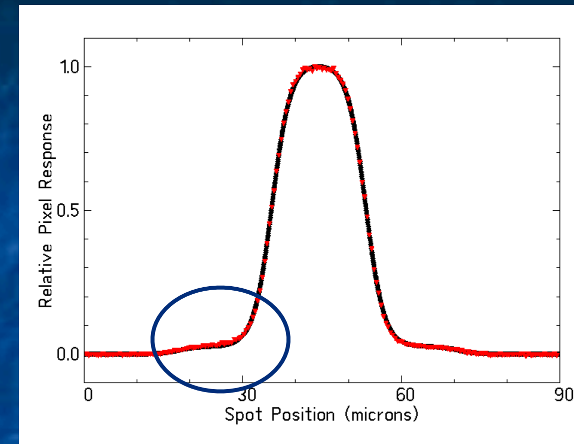

- Array of single pixel resets – can map out entire device quickly.

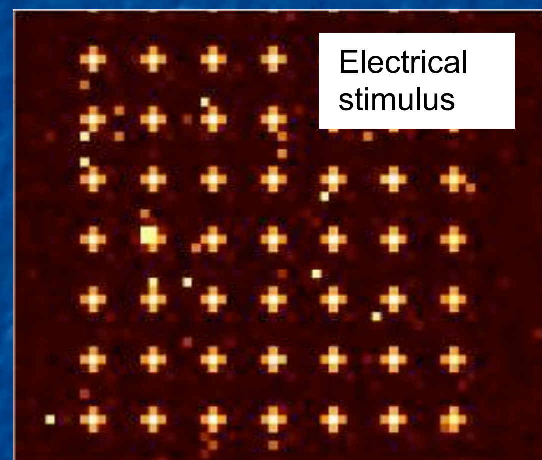

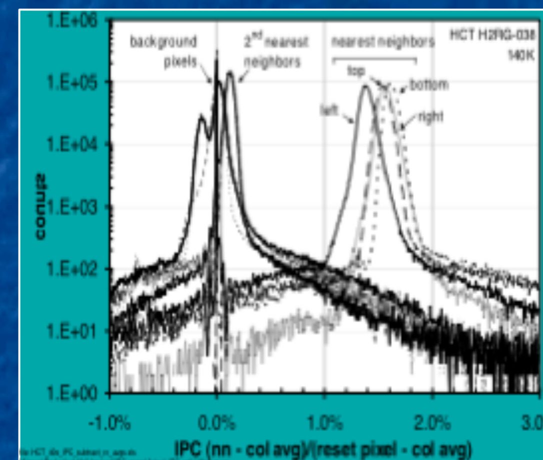

- Next generation device is a multi-pinhole projector. (see T. Biesiadzinski talk)

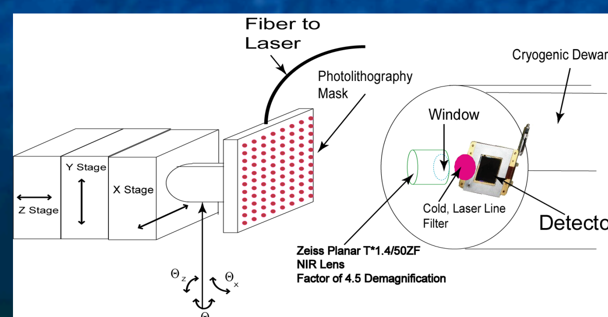

Persistence

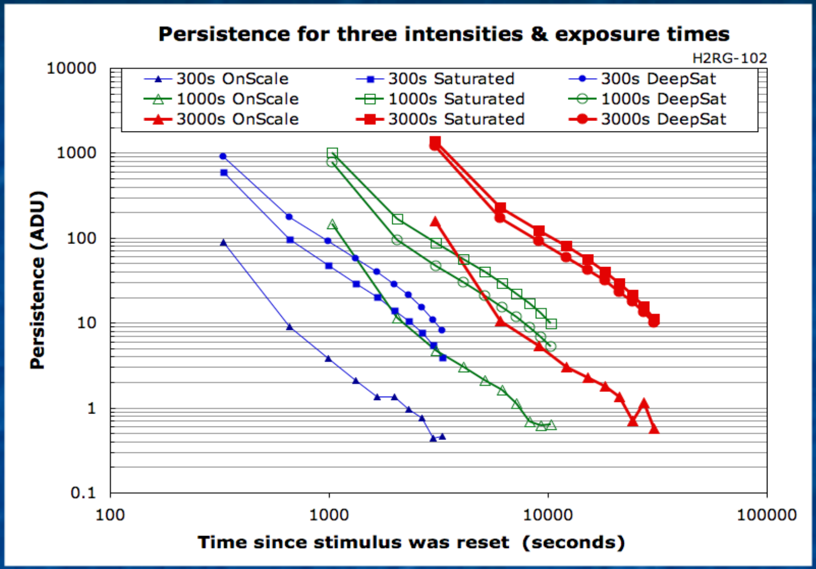

Persistence is present for any stimulus level.
For a given exposure time, it can be described as a % of the stimulus and the frame number following the stimulus.

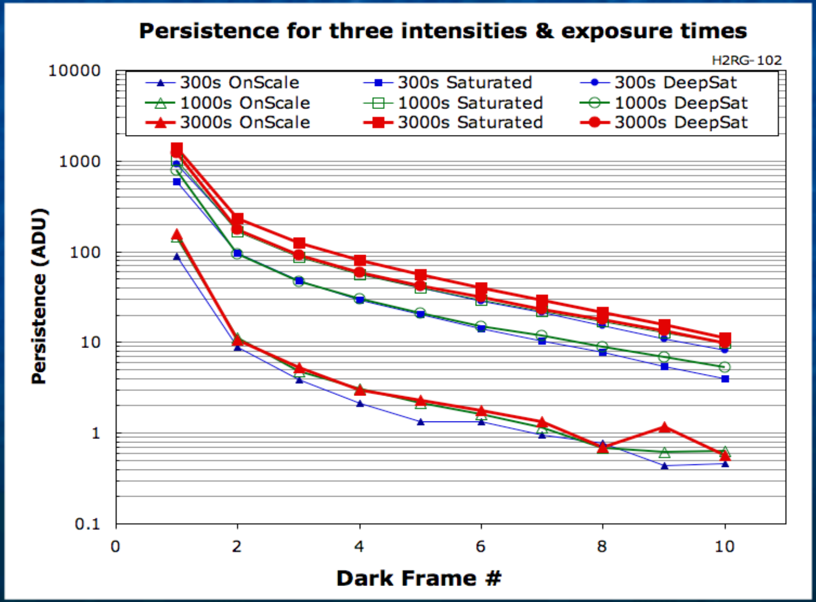

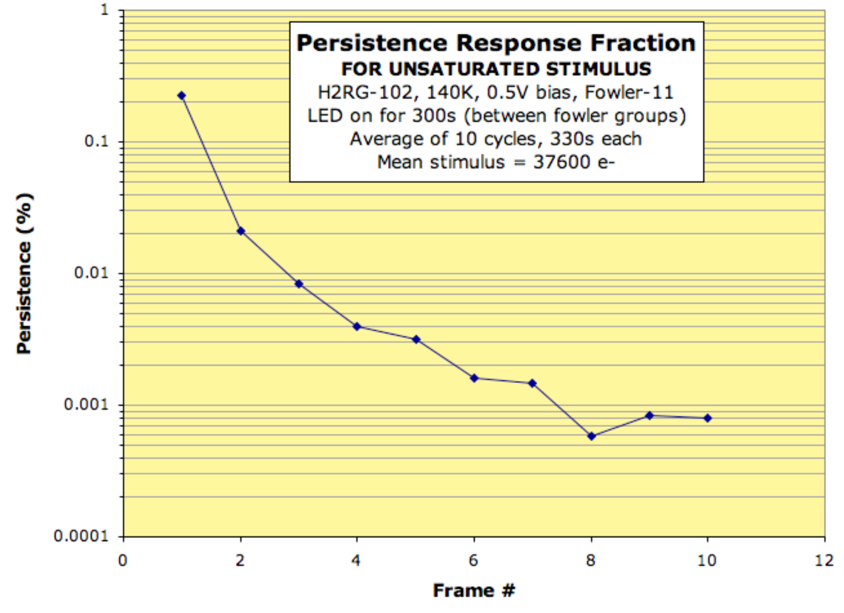

Reciprocity tests

Reciprocity failure if measured signal in the detector is not constant for all *Flux* and *Time* such that *Flux* x *Time* = constant.

- Reciprocity machine being commissioned
  - Monochromater illuminated pinholes calibrated to 0.2% per decade.
  - Pinholes span 5 decades in size.

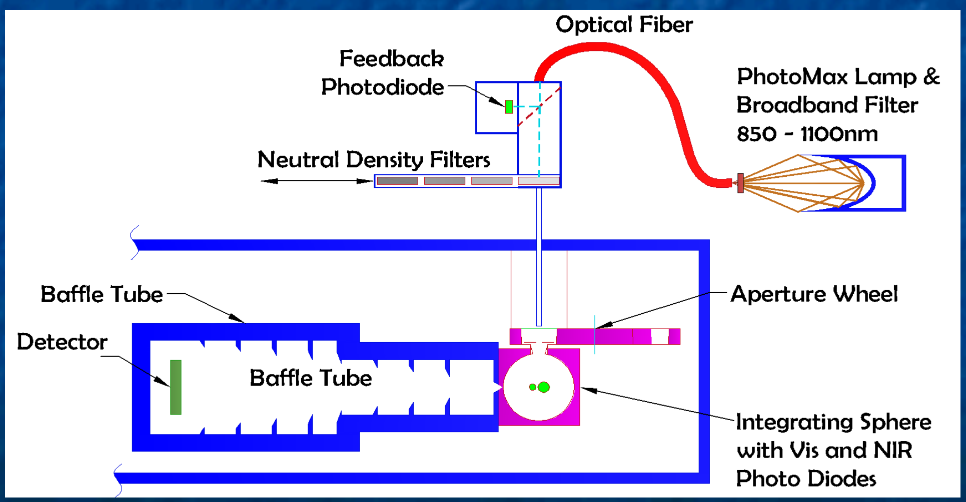

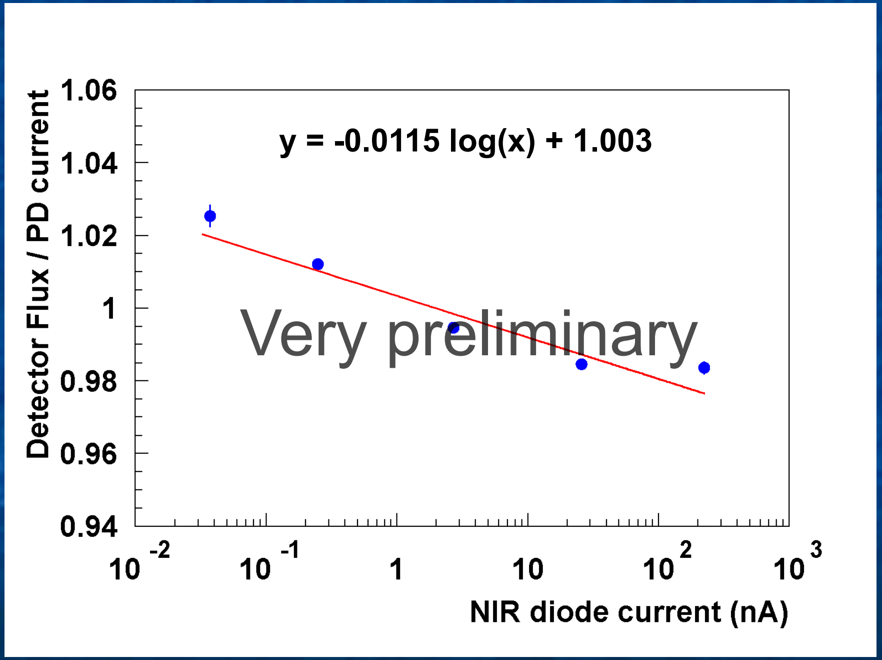

(see W. Lorenzon talk)

Full Field Image Projector

- Project known scene on CCD or NIR.
- Provide scientists (WL-ers in particular) with all known detectors effects.
- See with what precision the scene can be reconstructed.

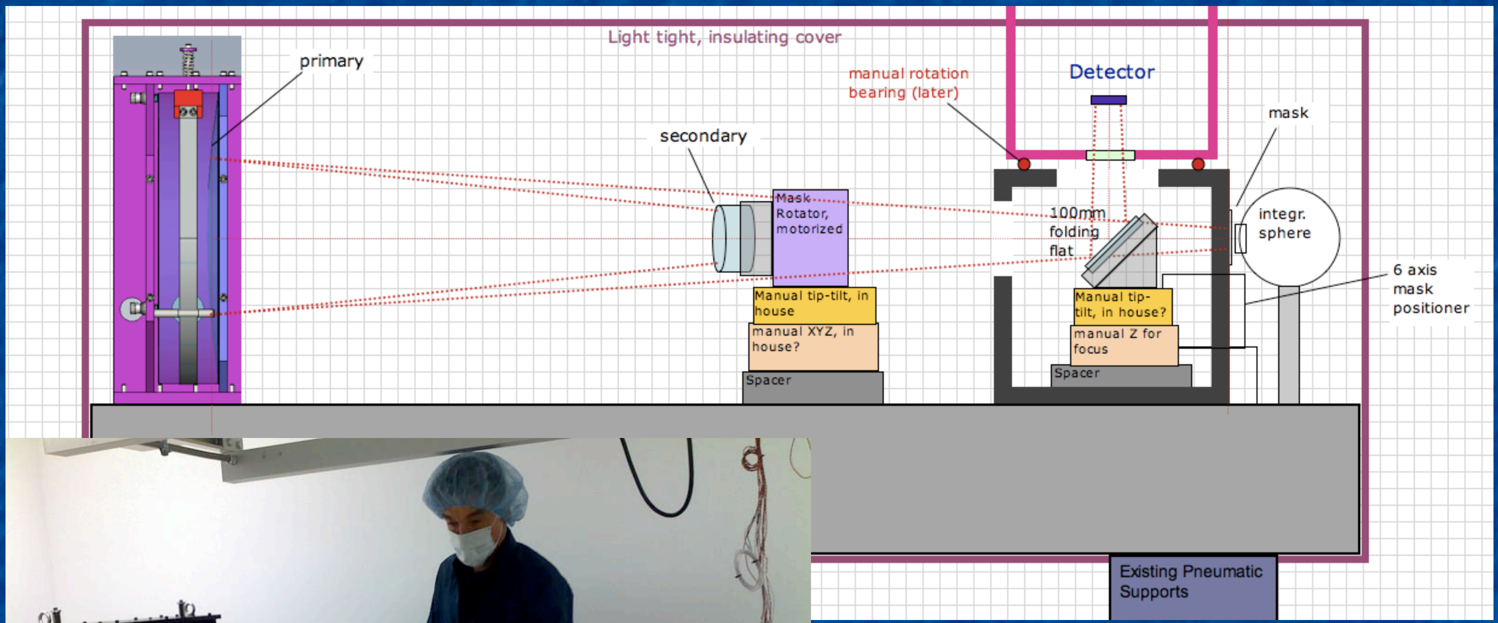

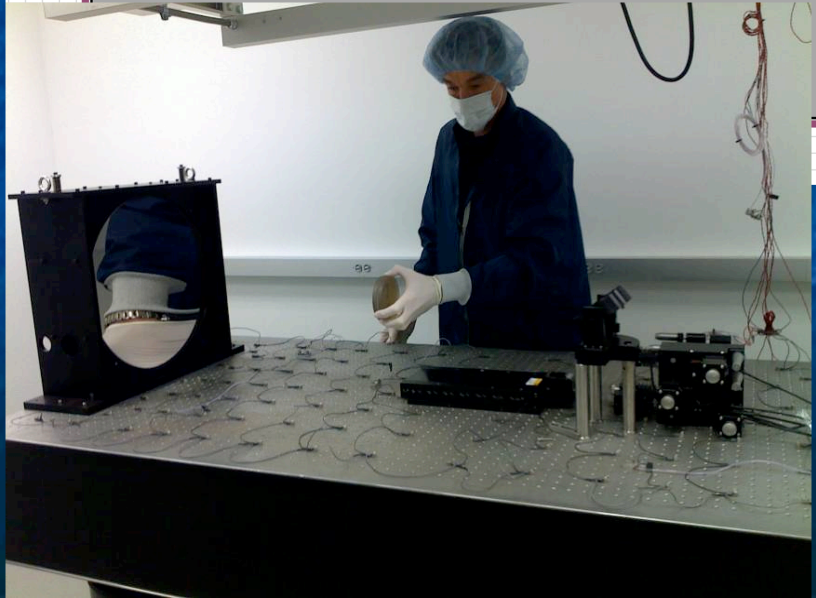

Electronics

NIR Frontend Electronics

(see P. Hart talk)

Teledyne SIDECAR ASIC

- Readout controller on a chip
- Developing our own programming and operational experience

SNAP packaging

- Supports direct connect to detector
- Supports 36-channel mode
- LVDS digital interface
- Four science data links
- Temperature monitoring
- Two delivered; four more in assembly

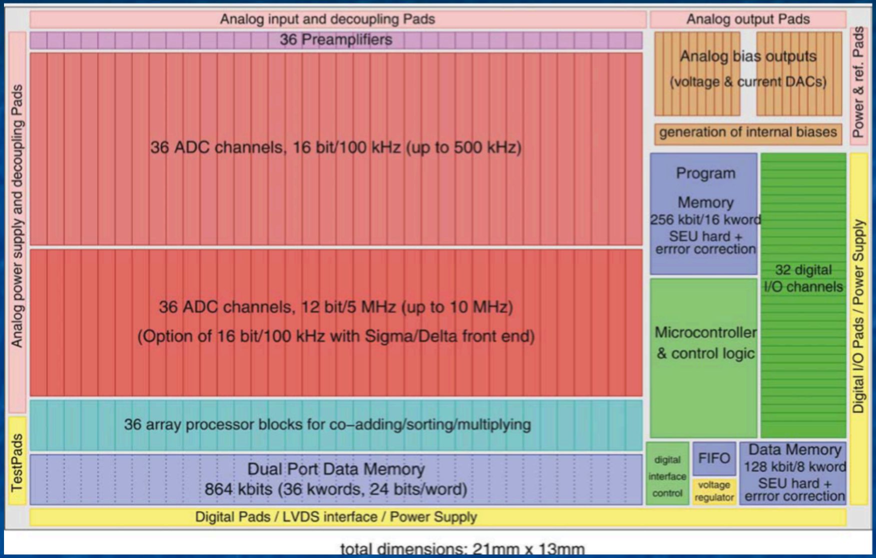

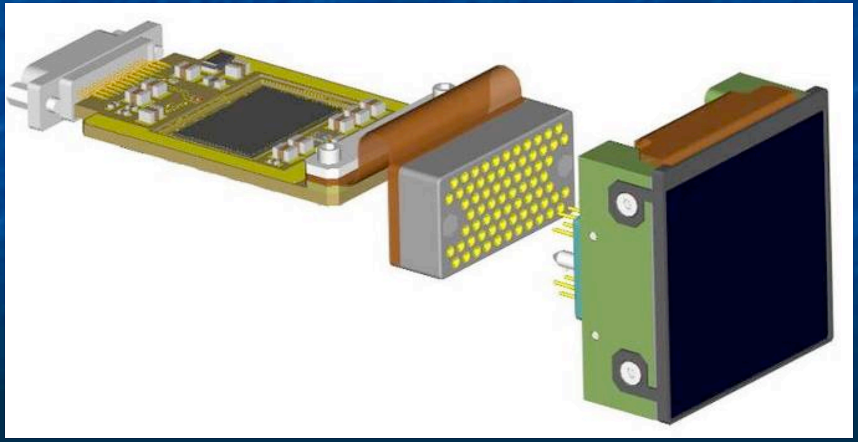

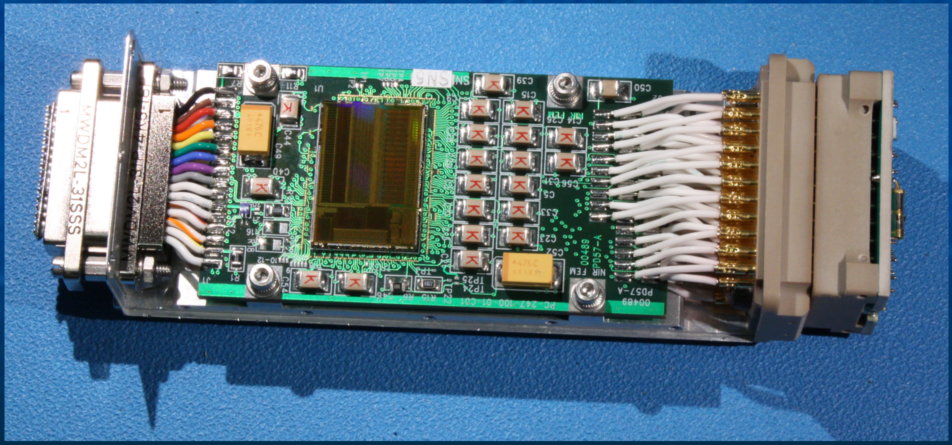

CCD Frontend Electronics

(see A. Karcher talk)

- Programmable biasing of CCD – -25V source follower biasing to +100V substrate bias
- Programmable clock levels
- Programmable clock pattern – special modes to support radiation damage monitoring
- Dual slope correlated double sampler and digitization of 4 CCD outputs
- Temperature monitoring – locally and at the CCD
- Same LVDS interface and protocol as SIDECAR ASIC (NIR)
- Designed for operation down to 120 K – verified
- Radiation tolerance design methodology – heavy ions testing at LBNL 88” Cyclotron

CLIC

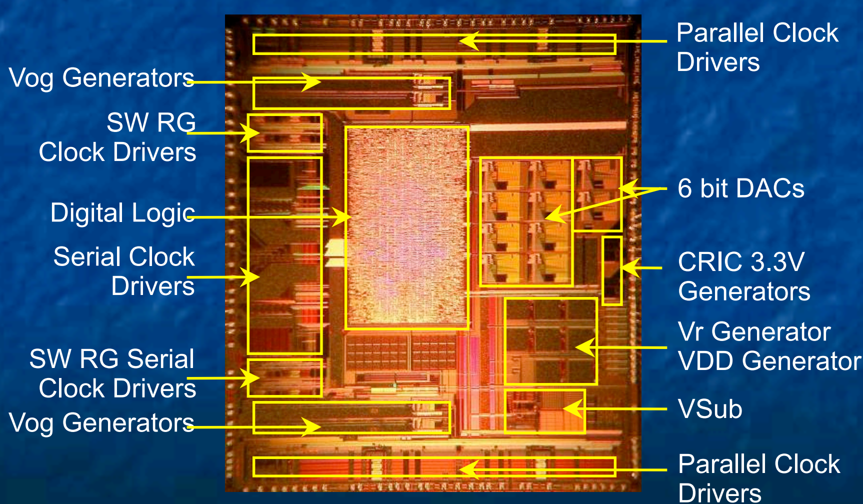

CRIC

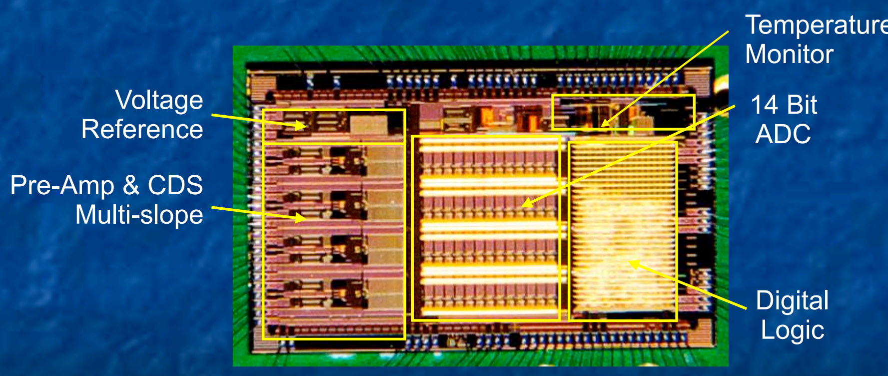

CCD Frontend Electronics

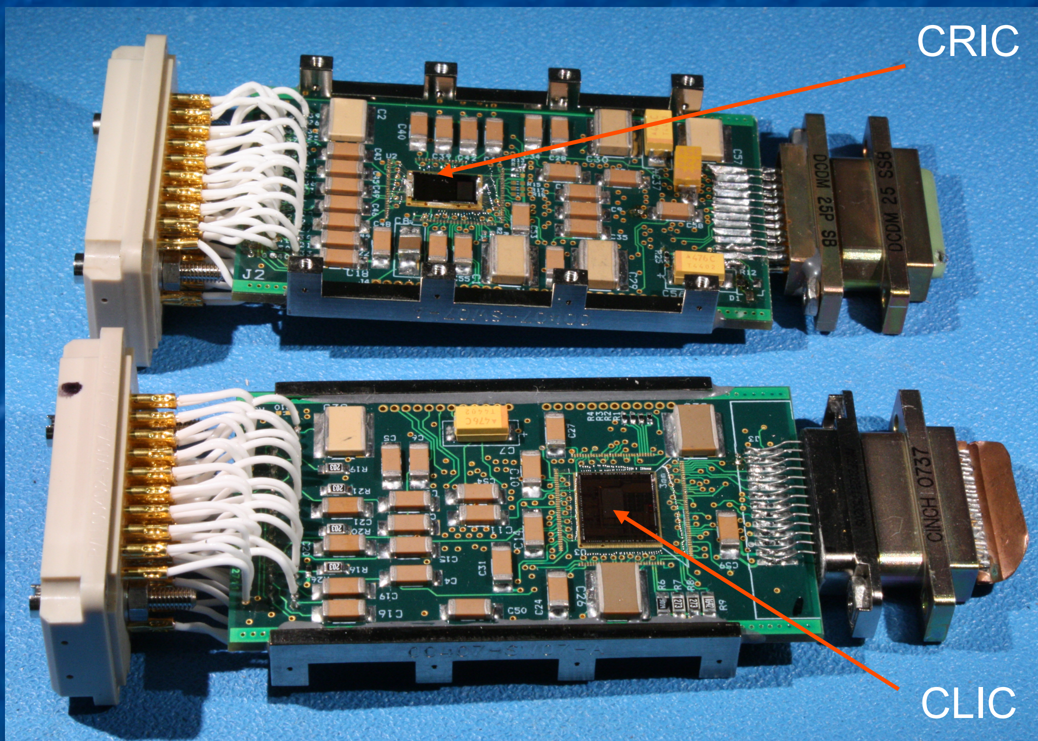

SNAP CCD and electronics at 140K

Flat field

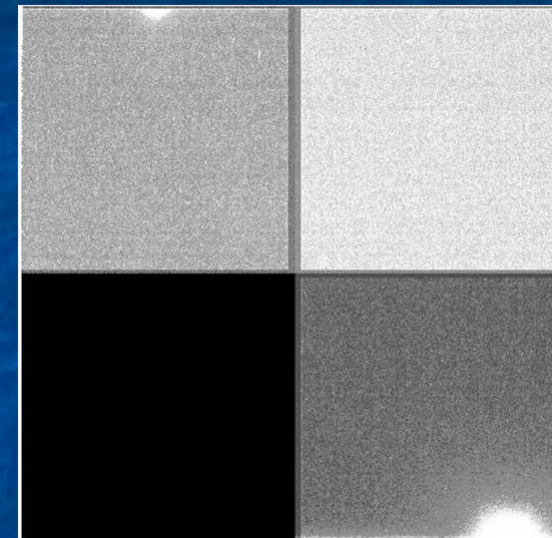

Tree image

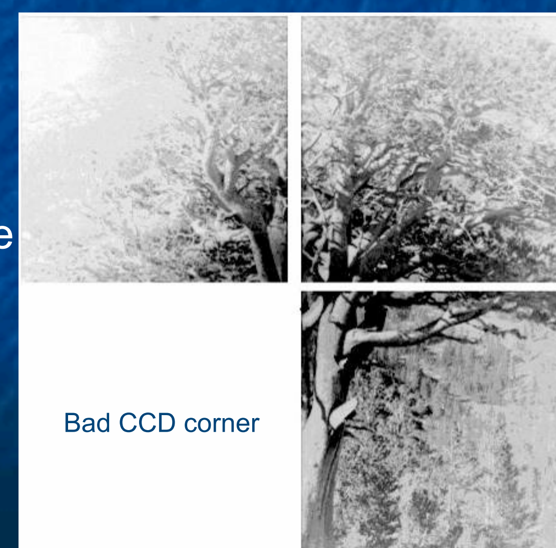

Data Control and Collection

(see P. Hart talk)

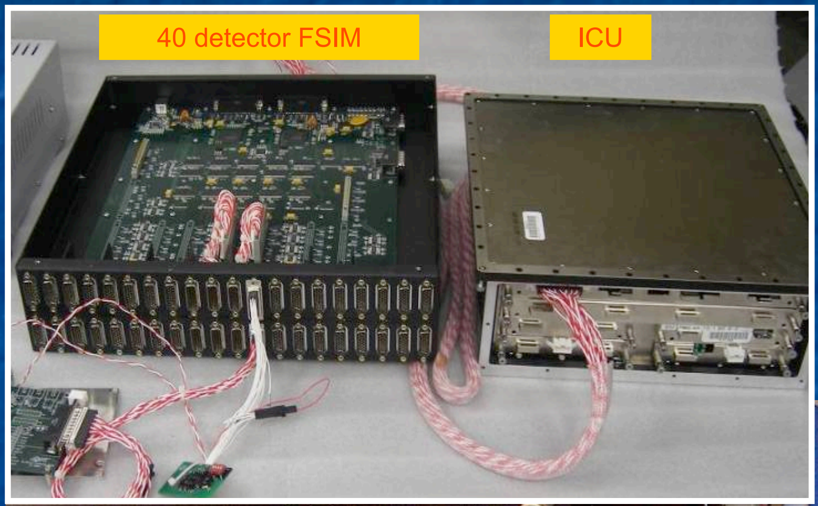

- Distributed detector electronics design makes for a light-weight data control and data collection system.
- Shown is system that handles 20 CCDs and 20 NIR.

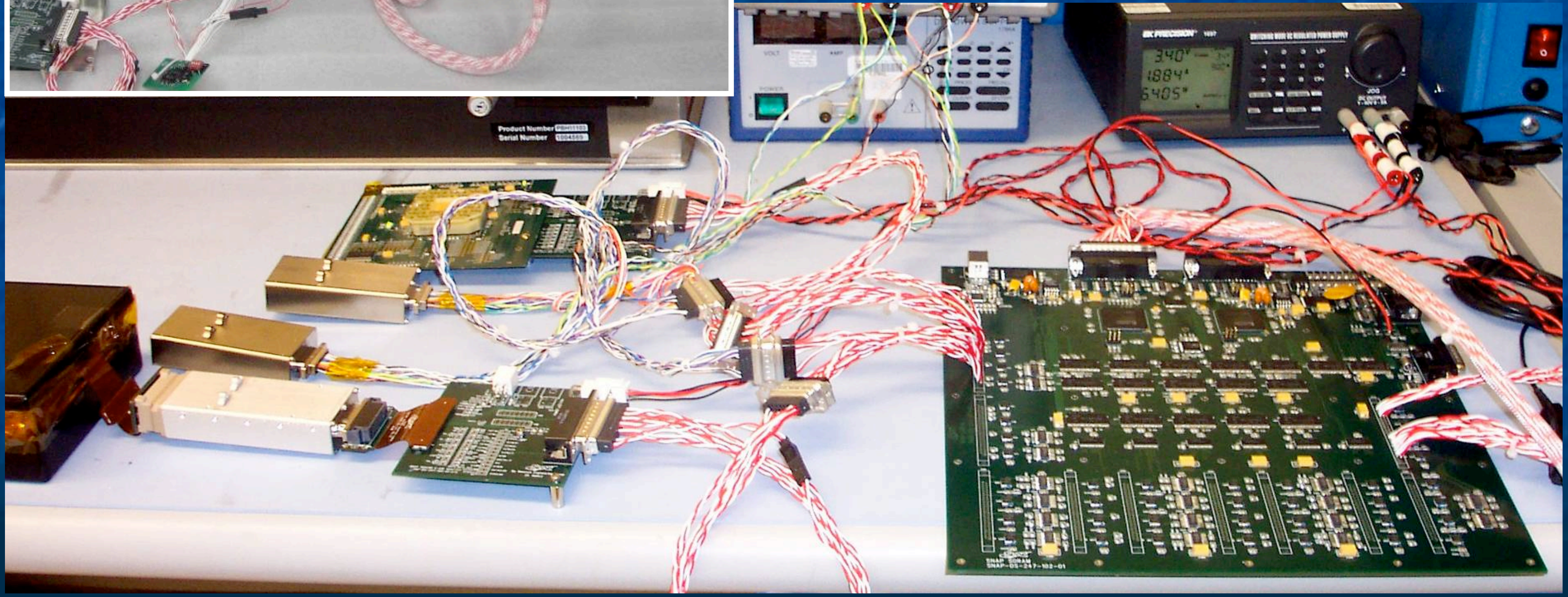

Building a Focal Plane

Drivers

- Use SiC for focal plane plate and detector mounts.
- Intermix NIR and VIS detectors in the focal plane.
- Detectors use 3-point mount.
- Detector mount designed for near 4-side abuttability
- Detector has space-rugged connector for blind mating of electronics.
- Excellent flatness of detector optical surface relative to mounting plane – flatness and height tolerance are built in, no shimming at integration.
- .....

CCD SiC Mounting

- SiC is good match to detector Si.
- Robust connector; blind mating to electronics box.
- Near four-side abuttable.
- Assembly evolved over 12 prototypes; production assembly underway.

CCD on SiC mount

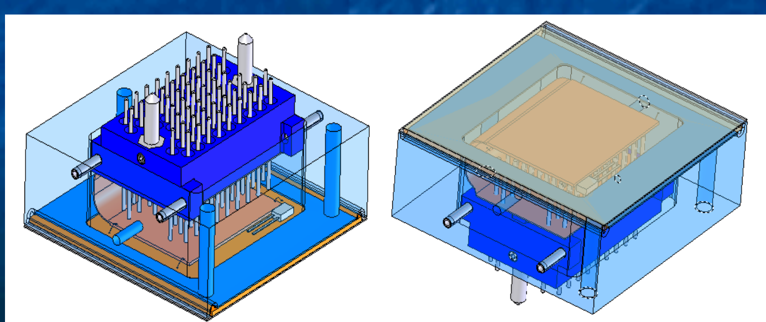

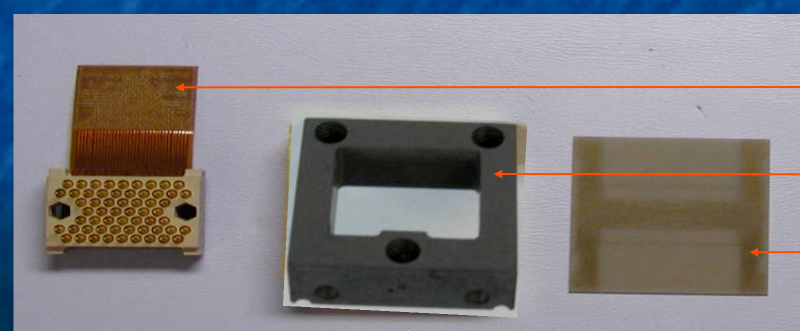

CCD SiC Mount Flatness

- One of the drivers for engineering the mounts was to meet stringent focal plane flatness tolerances – 10 μm (p-p) was.
- Total achieved flatness *at the detector material* is shown for three parts each.

CCD	
PP1	3 μm
PP2	6 μm
PP3	7 μm

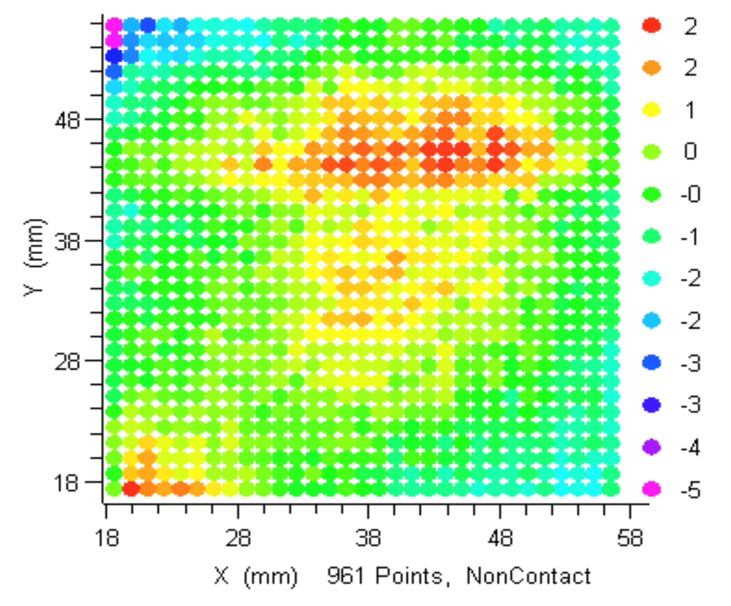

NIR SiC Mount

- SiC is good match to detector Si ROIC (readout IC).
- ROIC with attached detector material is directly glued to the SiC – no BCS (bonded composite structure).
- Robust connector; blind mating to electronics box.
- Near four-side abuttable.
- Low and high-speed 32-channel readout, reference pixels and window modes supported.

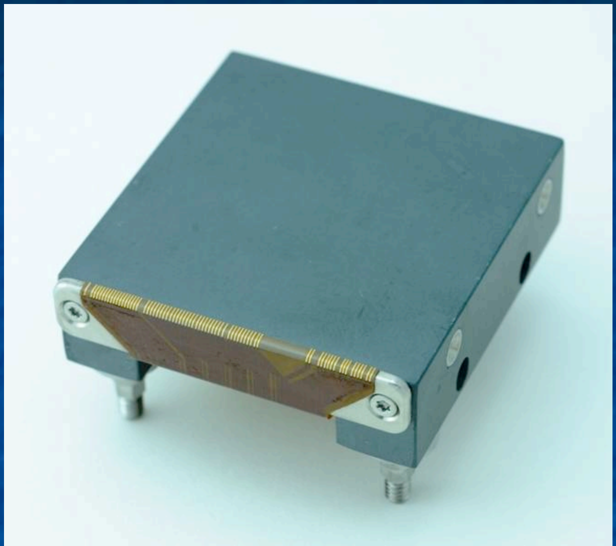

NIR SiC Mount Flatness

- One of the drivers for engineering the mounts was to meet stringent focal plane flatness tolerances – 20 μm (p-p) was allocated.
- Total achieved flatness *at the detector material* is shown for three parts.

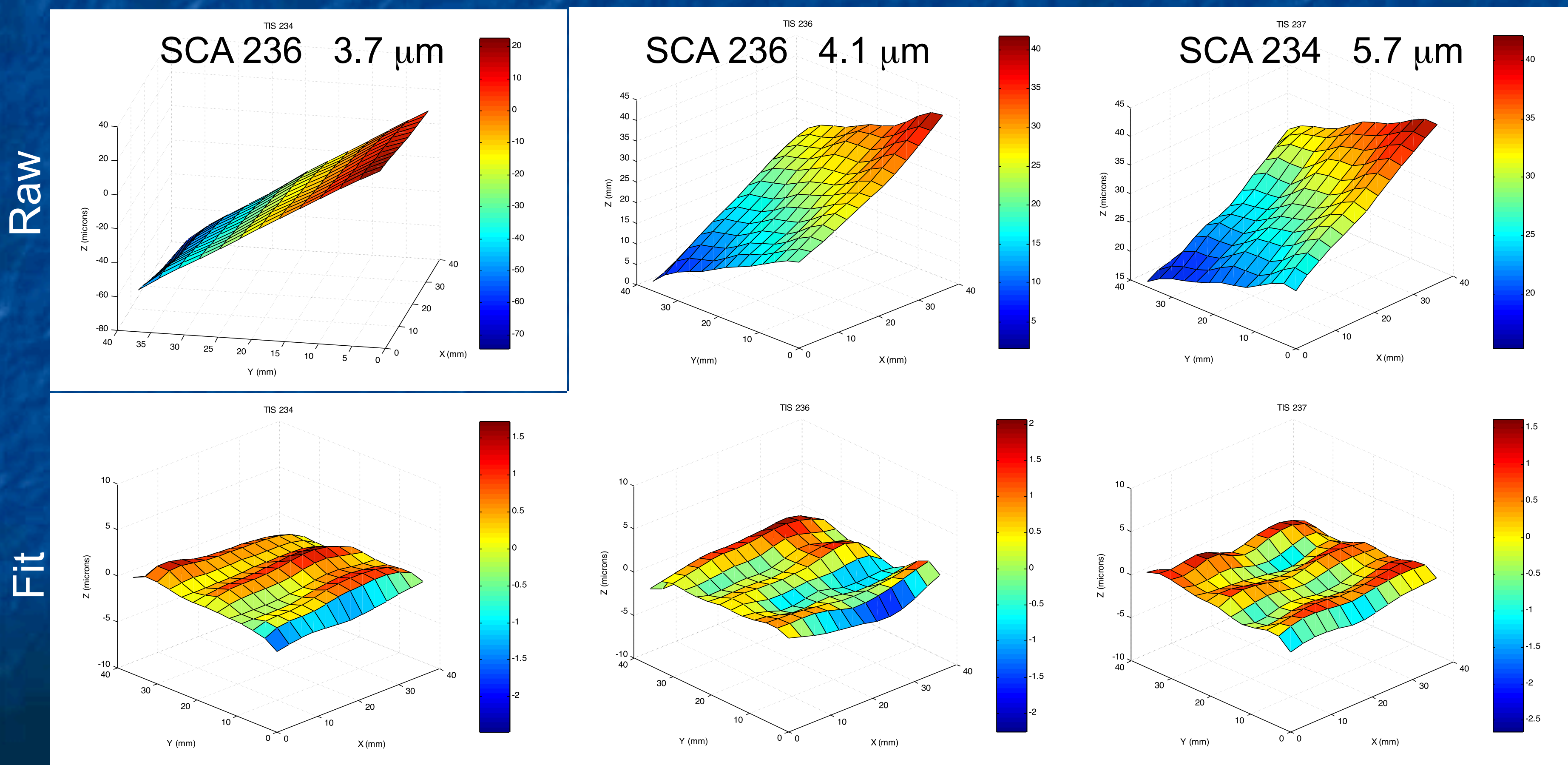

Bottom plots are deviation from best fit plane. The mounts provide this adjustment.

SiC Focal Plane

Demonstrator focal plane has shown:

- Precision SiC components are achievable - flatness to 2 μm.
- Metrology of focal plane, detectors, and assemblies meet flatness spec achievable *without* shimming.
- Position stability after vibration test of focal plane, mounts, and electronic module simulators.
- Thermal performance with simulated heat loads matches models.
- Position stability after thermal cycle test of focal plane, detectors, and electronic module simulators.

3x3 SiC demonstrator

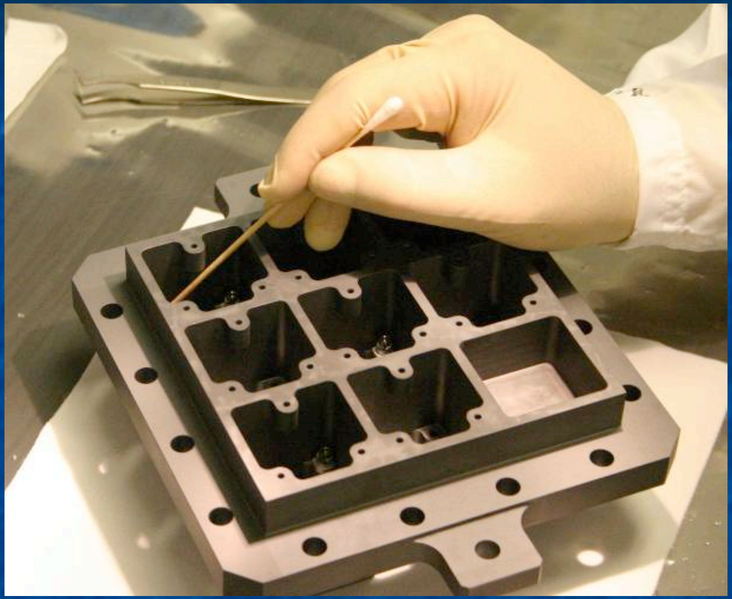

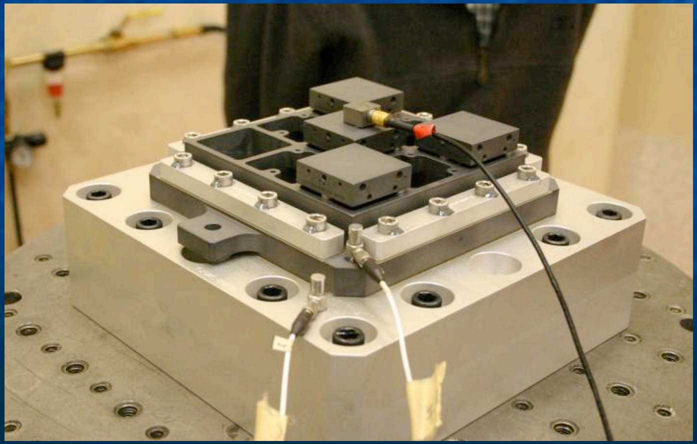

Instrumented for vibration test

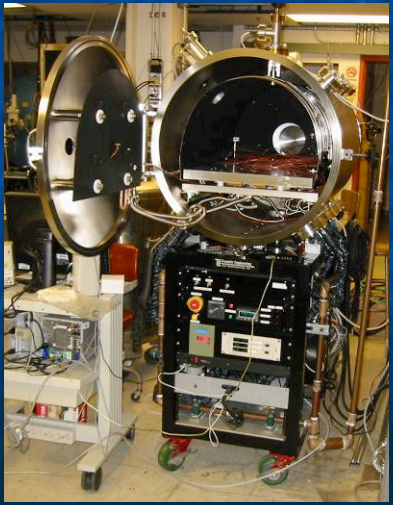

Thermal-vacuum

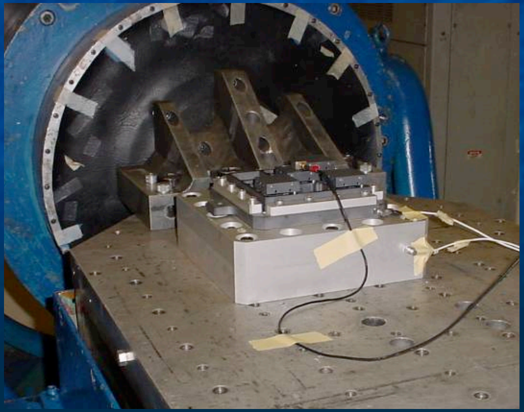

Mounted on vibration table

Demonstrator System

- Now that we have developed the parts, effort is shifting to system testing.
- Demonstrate interoperability of multiple NIR and CCDs, mixed or monotype.
- Look for crosstalk – understand grounding and cabling – underway as I speak.

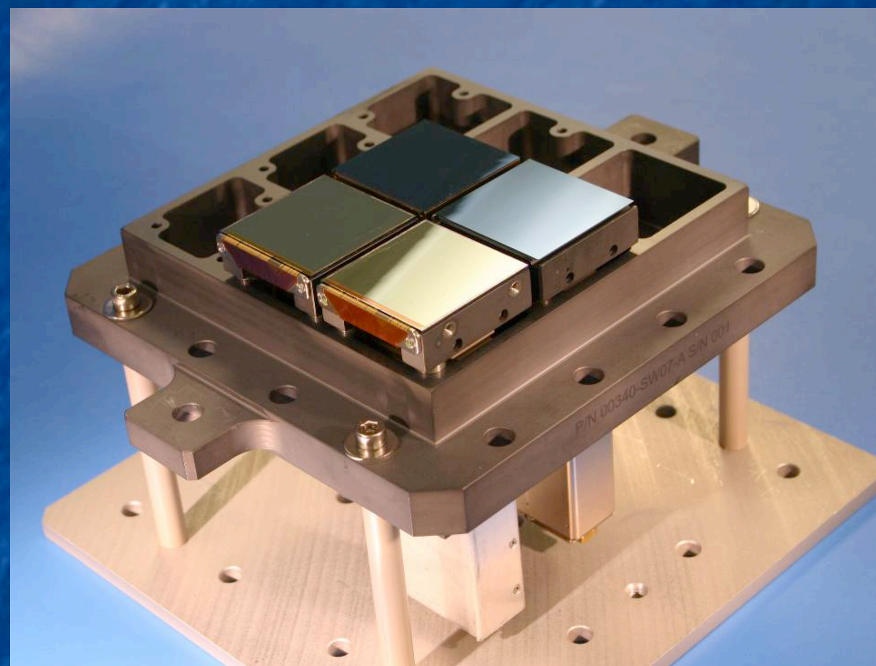

- Illustrated
  - Silicon carbide focal plane
  - Two CCDs and two NIR on SiC mounts.
  - Electronics modules directly attached.

Accomplishment Highlights

Detectors

- CCDs – radiation tolerant, fully depleted, good red response and small lateral charge diffusion.
- HgCdTe – 2k x 2k, 1.7 μm cutoff arrays.
- Cryogenic ASICs for CCD control and readout.
- Small footprint packaging for SIDECAR ASIC.
- SiC mounts for NIR and CCD enabling heterogeneous focal plane mosaic.

Characterization Techniques

- Virtual knife edge diffusion measurement for CCD.
- Multiple IPC measurement methods for NIR.
- Sub-pixel light beam mapping of intra and inter pixel response for CCD and NIR.
- Precision QE and reflectance measurements for CCD and NIR.
- Persistence analysis methods and model for NIR.
- Pixel response non-uniformity methods for CCD and NIR.
- Reciprocity measurement for NIR.
- Image projection and reconstruction of shapes coming for CCD and NIR.

Thank you

Recent NIR Papers

1. "Precision quantum efficiency measurements on 1.7 micron near infrared devices," M. Schubnell et al, Proc. SPIE 7021, (2008)
2. "Count rate dependent non-linearity and pixel size variations in 1.7 micron cut-off detectors," Wolfgang Lorenzon et al, Proc. SPIE 7021 (2008)
3. "Mapping electrical crosstalk in pixelated sensor arrays," S. Seshadri, D. M. Cole, B. R. Hancock, and R. M. Smith, Proc. SPIE 7021, 702104 (2008).
4. "Calibration of image persistence in HgCdTe photodiodes," Roger M. Smith, Maximilian Zavodny, Gustavo Rahmer, and Marco Bonati, Proc. SPIE 7021 (2008).
5. "A theory for image persistence in HgCdTe photodiodes," Roger M. Smith, Maximilian Zavodny, Gustavo Rahmer, and Marco Bonati, Proc. SPIE 7021 (2008).
6. "Comparing the low-temperature performance of megapixel NIR InGaAs and HgCdTe imager arrays," S. Seshadri et al, Proc. SPIE 6690, (2007)
7. "Image persistence in 1.7 µm cut-off HgCdTe focal plane arrays for SNAP," R. Smith et al, IEEE NSS '07, Volume 3, pp 2236 – 2245 (2007).
8. "Pixel area variation in CCDs and implications for precise photometric calibration," R. Smith et al, IEEE NSS '07 Volume 1, pp 429 - 435 (2007).
9. "Subpixel Response Measurement of Near-Infrared Detectors," N. Barron et al, PASP 119, pp 466–475 (2007).
10. "Correlated Noise and Gain in Unfilled and Epoxy-Underfilled Hybridized HgCdTe Detectors," M. Brown, M. Schubnell, and G. Tarlé, PASP 118, pp 1443–1447 (2006).
11. "Development of NIR detectors and science-driven requirements for SNAP," M. G. Brown et al, Proc. SPIE 6265 (2006)
12. "Characterization of NIR InGaAs imager arrays for the JDEM SNAP mission concept," S. Seshadri et al, Proc. SPIE 6276 (2006)
13. "Noise and zero point drift in 1.7µm cutoff detectors for SNAP," Roger Smith et al, Proc. SPIE 6276 (2006)
14. "Near infrared detectors for SNAP," M. Schubnell et al, Proc. SPIE 6276 (2006).
15. "Near infrared detectors for SNAP," M. Schubnell et al, Proc. SPIE 6276 (2006).
16. "Development of NIR detectors and science-driven requirements for SNAP, M G Brown et al, Proc. SPIE 6265 (2006).
17. "VIRGO-2K 2.25-µm HgCdTe dark current," R. Smith et al, Proc. SPIE 5499 (2004).
18. "SNAP Near Infrared Detectors," G. Tarle et al, Proc. SPIE 4850 (2003).

Recent CCD Papers

1. Stephen E. Holland, William F. Kolbe, and Christopher J. Bebek, “A 12.3 Mpixel, Fully Depleted, Back-Illuminated, High-Voltage Compatible Charge-Coupled Device For The SuperNova Acceleration Probe,” IEEE Trans. Elec. Dev. Special Issue on Image Sensors, (submitted).
2. Kyle Dawson, Chris Bebek, John Emes, Steve Holland, Sharon Jelinsky, Armin Karcher, William Kolbe, Nick Palaio, Natalie Roe, Juhi Saka, Koki Takasaki, and Guobin Wang, "Radiation Tolerance of Fully-Depleted p-Channel CCDs Designed for the SNAP Satellite," IEEE Trans. Nucl. Sci. 55, 1725-1735 (2008).
3. S. E. Holland, K. Dawson, N. P. Palaio, J. Saha, N. A. Roe, G. Wang, "Fabrication of back-illuminated, fully depleted charge-coupled devices," Nucl. Instrum. Methods A 579,, 653-657 (2007).
4. N. A. Roe, C. J. Bebek, K. S. Dawson, J. H. Emes, M. H. Fabricius, J. A. Fairfield, D. E. Groom, S. E. Holland, A. Karcher, W. F. Kolbe, et al., "Radiation-tolerant, red-sensitive CCDs for dark energy investigations," Nucl. Instrum. Methods A 572, 526-527 (2007).
5. Kyle Dawson, Chris Bebek, John Emes, Steve Holland, Sharon Jelinsky, Armin Karcher, William Kolbe, Nick Palaio, Natalie Roe, Koki Takasaki, and Guobin Wang, "Radiation Tolerance of High-Resistivity LBNL CCDs," IEEE NSS/ MIC 9872, 152-157 (2006) (San Diego).
6. S. E. Holland, C. J. Bebek, K. S. Dawson, J. H. Emes, M. H. Fabricius, J. A. Fairfield, D. E. Groom, A. Karcher, W. F. Kolbe, N. P. Palaio, N. A. Roe, & G. Wang, "High-voltage compatible, fully depleted CCDs," SPIE 6276, (May, 2006).
7. S. E. Holland, "Fully Depleted Charge-Coupled Devices," Proc. of the SNIC Symposium, Stanford, CA (3-6 April, 2006) [http://www.slac.stanford.edu/econf/C0604032/proceedings.htm]
8. Jessamyn A. Fairfield, D. E. Groom, S. J. Bailey, C. J. Bebek, S. E. Holland, A. Karcher, W. F. Kolbe, W. Lorenzon, & N. A. Roe, "Improved spatial resolution in thick, fully depleted CCDs with enhanced red sensitivity," IEEE Trans. Nucl. Sci. 53 (6), 3877-3881 (2006).
9. D. E. Groom, C. J. Bebek, M. Fabricius, A. Karcher, W.F. Kolbe, N. A. Roe, & J. Steckert, "Quantum efficiency characterization of back-illuminated CCDs Part 1: The Quantum Efficiency Machine," in SPIE 6068 (2006).
10. M. H. Fabricius, C. J. Bebek, D. E. Groom, A. Karcher, & N. A. Roe, "Quantum efficiency characterization of back-illuminated CCDs Part 2: Reflectivity measurements" in SPIE 6068 (2006).

Recent Electronics Papers

1. Integrating Signal Processing and A/D Conversion in One Focal-Plane Mounted ASIC, Turning photons into bits in the cold, A. Karcher et al, Scientific Detectors for Astronomy 2005, J. E. Beletic, J. W. Beletic, P. Amico editors, Springer (2006).
2. A Low Noise, Radiation Tolerant CCD Readout Processor for the Proposed SNAP Satellite, A. Karcher et al, IEEE Nuclear Science Symposium Conference Record, Oct. 2007, pp. 1069 – 1072.
3. A CCD clock controller ASIC using novel design techniques integrated in a CMOS 0.8mm SOI high voltage process, J.P. Walder et al, IEEE Nuclear Science Symposium Conference Record, Oct. 2007, pp 2404 – 2407.
4. A Precision Voltage and Current Reference for the SNAP CCD Readout IC, B. Krieger et al, IEEE Nuclear Science Symposium Conference Record, Oct. 2007, pp 2408 - 2410.